Published in final edited form as:
J Comp Neurol. 2010 January 10; 518(2): 229–253. doi:10.1002/cne.22228.

Collagen XIX Is Expressed by Interneurons and Contributes to the Formation of Hippocampal Synapses

Jianmin Su[1], **Karen Gorse**[1], **Francesco Ramirez**[2], and **Michael A. Fox**[1,*]

[1]Department of Anatomy and Neurobiology, Virginia Commonwealth University, Richmond, Virginia 23298

[2]Department of Pharmacology and Systems Therapeutics, Mount Sinai School of Medicine, New York, New York 10029

Abstract

Extracellular matrix (ECM) molecules contribute to the formation and maintenance of synapses in the mammalian nervous system. We previously discovered a family of nonfibrillar collagens that organize synaptic differentiation at the neuromuscular junction (NMJ). Although many NMJ-organizing cues contribute to central nervous system (CNS) synaptogenesis, whether similar roles for collagens exist at central synapses remained unclear. In the present study we discovered that *col19a1*, the gene encoding nonfibrillar collagen XIX, is expressed by subsets of hippocampal neurons. Colocalization with the interneuron-specific enzyme glutamate decarboxylase 67 (Gad67), but not other cell-type-specific markers, suggests that hippocampal expression of *col19a1* is restricted to interneurons. However, not all hippocampal interneurons express *col19a1* mRNA; subsets of neuropeptide Y (NPY)-, somatostatin (Som)-, and calbindin (Calb)-immunoreactive interneurons express *col19a1*, but those containing parvalbumin (Parv) or calretinin (Calr) do not. To assess whether collagen XIX is required for the normal formation of hippocampal synapses, we examined synaptic morphology and composition in targeted mouse mutants lacking collagen XIX. We show here that subsets of synaptotagmin 2 (Syt2)-containing hippocampal nerve terminals appear malformed in the absence of collagen XIX. The presence of Syt2 in inhibitory hippocampal synapses, the altered distribution of Gad67 in collagen XIX-deficient subiculum, and abnormal levels of gephyrin in collagen XIX-deficient hippocampal extracts all suggest inhibitory synapses are affected by the loss of collagen XIX. Together, these data not only reveal that collagen XIX is expressed by central neurons, but show for the first time that a nonfibrillar collagen is necessary for the formation of hippocampal synapses.

INDEXING TERMS

extracellular matrix; collagen; synaptogenesis; hippocampus; interneuron

Synapse formation is a multistep process orchestrated by developmentally regulated signals that are either passed between putative synaptic partners or present in the extracellular environment. Initial advances in identifying synaptic organizing signals came from studies of the accessible neuromuscular junction (NMJ), where extracellular factors embedded in the basal lamina separating motor nerve terminals from postsynaptic muscle membrane were sufficient to induce synaptogenesis (Sanes et al., 1978; Burden et al., 1979; for review, see

*CORRESPONDENCE TO: Michael A. Fox, 1101 East Marshall Street, Richmond, VA 23298-0709. mafox@vcu.edu.

Additional Supporting Information may be found in the online version of this article.

Sanes and Lichtman, 1999; Fox and Umemori, 2006). Biochemical, molecular, and genetic studies have since identified roles for agrin, laminin α chains, and Wnts in the organization of the postsynaptic apparatus (Nitkin et al., 1987; Gautam et al., 1996; Sanes and Lichtman, 1999; Burgess et al., 1999; Lin et al., 2001, 2005; Misgeld et al., 2005; Kummer et al., 2006; Nishimune et al., 2008; Henriquez et al., 2008) and collagen IV, laminin β2, and fibroblast growth factors (FGFs) in the formation of presynaptic terminals (Noakes et al., 1995; Nishimune et al., 2004; Fox et al., 2007). In contrast to the NMJ, narrow synaptic clefts and lack of basal laminae in the central nervous system (CNS) initially suggested that pre- and postsynaptic transmembrane molecules directed both the targeting and formation of central synapses. Indeed, several families of transmembrane adhesion molecules, including cadherins, protocadherins, NCAM, SynCAMs, dsCAMs, sidekicks, SALMs, nectins, neuroligins, neurexins, integrins, ephrins, and Eph receptors, are present at central synapses and have been implicated in synaptic targeting, differentiation, or maintenance (Yamagata et al., 2003; Scheiffele, 2003; Gerrow and El-Husseini, 2006; Fox and Umemori, 2006; Craig et al., 2006; Craig and Kang, 2007; Dalva et al., 2007; Sanes and Yamagata, 2009). More recently, however, it has been demonstrated that extracellular molecules, including growth factors, morphogens, proteolytically shed transmembrane molecules, and bulkier matrix molecules, also contribute to central synaptogenesis (e.g., O'Brien et al., 1999, 2002; Hall et al., 2000; Umemori et al., 2004; Christopherson et al., 2005; Bjartmar et al., 2006; Stevens et al., 2007; Umemori and Sanes, 2008). These findings raise the possibility that NMJ-organizing molecules may also contribute to the formation of central synapses. Indeed, agrin, laminins, Wnts, and FGFs each contribute to central synaptogenesis (Libby et al., 1999; Hall et al., 2000; Bose et al., 2000; Umemori et al., 2004; Ksiazek et al., 2007; Egles et al., 2007; Davis et al., 2008). However, one family of NMJ organizing molecules, nonfibrillar collagens, has yet to be examined for its potential role in the formation of central synapses.

Nonfibrillar collagens have presumably been overlooked for CNS functions due to the widely held belief that the mammalian CNS lacks collagen, with the exception of that associated with vascular structures (Gallyas et al., 1970). Although early biochemical and histological studies demonstrated few collagen fibers in mammalian CNS tissue (e.g., Lowry et al., 1941), it is now clear that not all collagens are assembled into collagen fibers. In fact, while mammals express 45 collagen genes, fewer than 15 of these genes generate fibrillar collagen (Myllyharju and Kivirikko, 2004; Kadler et al., 2007; Fox, 2008). Despite not being assembled into fibers, CNS expression and function of nonfibrillar collagens still has received little attention (but see Sumiyoshi et al., 2001, Sund et al., 2001, Hashimoto et al., 2002, Claudepierre et al., 2005; Koch et al., 2006, Veit et al., 2006; Seppanen et al., 2007, Hubert et al., 2009). On the basis of collagen function at peripheral synapses, we examined the expression and function of *col19a1*, the gene encoding nonfibril-forming collagen XIX (Yoshioka et al., 1992; Myers et al., 1993, 1994; Inoguchi et al., 1995) in mouse hippocampus. We focused on hippocampus because its circuitry, cell types, and synaptic morphologies have been well documented (Fig. 1A) (Danglot et al., 2006; Klausberger and Somogy, 2008).

Collagen XIX, although initially identified as a fibrilassociated collagen with interrupted triple helices (FACIT) by sequence analysis (Khaleduzzaman et al., 1997), does not appear to bind collagen fibers but rather accumulates in the extracellular matrix (ECM) of restricted tissues, including neural tissue (Myers et al., 1997; Sumiyoshi et al., 1997, 2001). Aggregates of collagen XIX have been proposed to modulate cell-matrix interactions and cell-cell communication (Myers et al., 2003). In esophageal muscle, collagen XIX is essential for both muscle physiology and differentiation (Sumiyoshi et al., 2004). Proper formation of a collagen XIX-rich basal lamina is required for nitric oxide (NO)-dependent relaxation of lower esophageal sphincter (LES) muscle, perhaps as a result of a disorganized

basal lamina at LES neuromuscular junctions (Sumiyoshi et al., 2004). More recently, the noncollagenous 1 (NC1) domain of collagen XIX was shown to exhibit bioactivities similar to collagens IV NC1 domains (Kalluri, 2003; Ramont et al., 2007). Since collagen IV NC1 domains act as presynaptic organizing molecules at the NMJ (Fox et al., 2007), we examined hippocampal nerve terminals in previously generated mutants lacking collagen XIX (Sumiyoshi et al., 2004). Although hippocampal organization appears grossly normal in these mutants, striking presynaptic defects were observed in the subiculum of the hippocampus, suggesting collagen XIX is necessary for the assembly of some hippocampal synapses.

MATERIALS AND METHODS

Animals

CD1 and C57BL/6 mice embryos were obtained from Charles River Laboratories (Wilmington, MA). The generation of collagen XIX null mice (*col19a1*$^{-/-}$; previously referred to as N19) was previously described (Sumiyoshi et al., 2004). Mutant mice were backcrossed for > 10 generations on C57BL/6 mice. Genomic DNA was isolated from tail using the HotSHOT method (Truett et al., 2000) and genotyping was performed with the following primers: *lacZ* 5′-TTC ACT GGC CGT CGT TTT ACA ACGTCG TGA-3′ and 5′-ATG TGA GCG AGT AAC AAC CCG TCG GAT TCT-3′; *col19a1 (exon4)* 5′-CTTCGC AAAACG CATGCCTCAGA-3′ and 5′-TTG TTC GTT TGT TTG TTT TTA ATC AAT CAA-3′. The following cycling conditions were used on an Eppendorf Mastercycler EP: 95°C for 5 minutes, followed by 35 cycles of amplification (95°C for 30 seconds, 52°C for 30 seconds, 72°C for 45 seconds), and 10 minutes at 72°C. All analyses conformed to National Institutes of Health (NIH) guidelines and were carried out under protocols approved by the Virginia Commonwealth University (VCU) Institutional Animal Care and Use Committee.

Reagents

All chemicals and reagents were obtained from either Sigma (St. Louis, MO) or Fisher (Fairlawn, NJ), unless otherwise noted.

Antibodies

Monoclonal and polyclonal antibodies used in these studies are listed and described in Table 1. Fluorescently conjugated secondary antibodies were obtained from Molecular Probes/Invitrogen (Eugene, OR) and were applied at a 1:1,000 dilution. Horseradish peroxidase (HRP)-conjugated secondary antibodies were from Jackson ImmunoResearch Laboratories (West Grove, PA) and were used at 1:10,000 dilutions. Alkaline phosphatase- and HRP-conjugated anti-DIG or anti-fluorescein antibodies were obtained from Roche (Mannheim, Germany) and were used at 1:1,000.

The following are characterizations of antibodies applied in the present studies.

Actin—The mouse anti-actin monoclonal antibody detects a 42-kDa band in Western blots of various vertebrate tissues, including mouse hippocampus and rat forebrain (shown here; Otey et al., 1987; Sano et al., 2006; Cowell et al., 2007).

Calbindin—The calbindin D-28k antibody recognizes a single band of ≈28 kDa on Western blots of mouse and rat brain extracts (see manufacturer's datasheet) and stained cells in the rodent hippocampus that were identical to previous reports (Sloviter, 1989; Danglot et al., 2006; Klausberger and Somogyi, 2008). Immunoreactivity of anti-calbindin

in immunohistochemistry (IHC) was marginally enhanced following in situ hybridization (ISH) (Supporting Fig. 1; see also Fig. 3).

Calretinin—The calretinin antibody recognizes a single band of ≈30 kDa on Western blots with mouse hippocampal extracts (unpubl. obs., J.S. and M.A.F.) and stained cells in the mouse hippocampus and cortex that were identical to previous reports (Liu et al., 2003; Xu et al., 2004; Danglot et al., 2006; Klausberger and Somogyi, 2008). Immunoreactivity of anti-calretinin in IHC was marginally enhanced following ISH (Supporting Fig. 1).

Gad65/67—The Gad65/67 antibody detects a doublet of ≈65 and 68 kDa in Western blots of rat brain extracts; immunoreactivity of the Gad65/67 antibody was abolished by preincubating with the immunizing peptide (manufacturer's datasheet). Previous IHC studies demonstrated that this antibody specifically labeled interneurons and inhibitory synapses in rat suprachiasmatic nuclei (Belenky et al., 2008).

Gad67—The Gad67 antibody detects a single band of ≈68 kDa in rat and mouse brain extracts and has no detectable cross-reactivity with Gad65 (manufacturer's datasheet; see also Varea et al., 2005). Previous IHC studies demonstrated that this antibody labels interneurons and inhibitory synapses in mouse cortex (Xu et al., 2006). Here, IHC with anti-Gad67 labeled similar, albeit fewer, interneurons and synaptic structures in hippocampus as anti-Gad65/67 (see Fig. 12).

Gephyrin: The gephyrin monoclonal antibody detects the 93-kDa isoform of gephyrin in mouse hippocampal and rat forebrain extracts (shown here; Henny and Jones, 2006). This antibody labels postsynaptic structures at inhibitory synapses in IHC of rat forebrains (Henny and Jones, 2006).

Iba-1: The Iba-1 antibody detects microglia and macrophages but not neural cells (see manufacturer's datasheet). In our hands this antibody labeled small cells in mouse hippocampus that resembled microglia, which matched previous descriptions (Imai et al., 1996).

NeuN: The NeuN antibody detects an uncharacterized nuclear protein present in most vertebrate neurons (Mullen et al., 1992). In our hands this antibody stains a pattern of cells in mouse hippocampus identical with previous reports (e.g., Mullen et al., 1992). In Western blots, the NeuN antibody detects two bands of 46 and 48 kDa (Mullen et al., 1992).

Neuropeptide Y (NPY): In IHC the NPY antibody labels subsets of cortical and hippocampal interneurons that were distributed as previously reported (Xu et al., 2004; Danglot et al., 2006; Klaus-berger and Somogyi, 2008). IHC with this antibody was blocked by preincubation with excess NPY, but not other related peptides such as peptide YY (manufacturer's datasheet). Importantly, this antibody worked poorly with our standard IHC protocol; however, immunolabeling was enhanced after ISH (Supporting Fig. 1).

PSD-95: The PSD-95 antibody detects a single 95-kDa protein in Western blots of mouse hippocampus (shown here; see also Kornau et al., 1995; Henny and Jones, 2006). This antibody labels postsynaptic densities in IHC of rat forebrains (Henny and Jones, 2006).

Somatostatin (Som): In IHC the Som antibody labels subsets of interneurons that were distributed as previously reported in mouse hippocampus, cortex, and retina (Oliva et al., 2000; Xu et al., 2004, 2006; Danglot et al., 2006; Klausberger and Somogyi, 2008; Acosta et al., 2008). Previous studies demonstrated that immunoreactivity was inhibited by

preincubation with nonlabeled somatostatin (Arimura et al., 1975). Importantly, this antibody worked poorly with our standard IHC protocol; however, immunolabeling was enhanced after ISH (Supporting Fig. 1).

Syt2: The Syt2 antibody, called *znp1*, was identified in a screen for tissue-specific antibodies in zebrafish (Trevarrow et al., 1990) and was recently shown to detect mouse Syt2 by both Western blot and IHC (Fox and Sanes, 2007). In Western blots of mouse cerebellum, hippocampi, and synaptosome fractions this antibody detects a single band at 60 kDa (Fox and Sanes, 2007; see also Fig. 10). Protein immunoprecipitated with this antibody was identified as Syt2 by mass spectrometry and Western blots demonstrated that this antibody specifically detected recombinant Syt2 but not Syt1, a closely related family member (Fox and Sanes, 2007).

Synapsin: The synapsin antibody detects a single ≈75-kDa protein in Western blots of mouse brain synaptosome fractions (Fox and Sanes, 2007) or mouse hippocampal extracts (shown here). In IHC, this antibody labels nerve terminals at the mouse NMJ and in mouse hippocampus (Fox et al., 2007; Armstrong et al., 2006).

VGlut1 and VGlut2: In Western blots, the VGlut1 antibody detects a single smeared band of 45–55 kDa and the VGlut2 antibody detects a single band at 60 kDa (shown here). In IHC these antibodies exhibit unique immunoreactivities in mouse hippocampus (manufacturer's data sheet); these patterns match previous descriptions of VGlut1 and VGlut2 distribution in mouse hippocampus (Herzog et al., 2006).

Collagen XIX: In addition to the antibodies used here, we tested commercial collagen XIX antibodies (from Abnova, Walnut, CA, and Santa Cruz Biotechnology, Santa Cruz, CA). Neither appeared specific to mouse collagen XIX protein in Western blots or IHC when compared with reactivity with collagen XIX-deficient tissue (unpubl. obs., J.S. and M.A.F.). For this reason, collagen XIX IHC was omitted from the current study.

IHC

Mouse brains were fixed in 4% paraformaldehyde (PFA) (in phosphate-buffered saline, PBS) for 12 hours at 4°C, then washed in PBS several times and incubated for at least 24 hours in 20% sucrose in PBS. Fixed tissue was frozen in Tissue Freezing Medium (Triangle Biomedical Sciences, Durham, NC), and 10–16-μm sections were cut on a Leica CM1850 cryostat. Sections were allowed to air dry for 15 minutes before being incubated with blocking buffer (2.5% normal goat serum, 2.5% bovine serum albumin, 0.1% Triton X-100 in PBS) for 30 minutes. Primary antibodies, diluted in blocking buffer, were incubated on tissue sections for 12 hours at 4°C. After washing in PBS, secondary antibodies, diluted in blocking buffer, were applied to the slides for 1 hour at room temperature. Tissue sections were washed thoroughly with PBS, coverslipped with VectaShield (Vector Laboratories, Burlingame, CA), and visualized on a Leica SP2 scanning confocal microscope or a Zeiss AxioImager A1 fluorescent microscope. When comparing mutant and control age-matched samples images were acquired by confocal microscopy using identical parameters (i.e., identical objective, zoom, laser intensity, gain, offset, scan speed, step size, and number of z-stacks) optimized for control tissues. Average fluorescent intensities were determined with Metamorph on maximum projection images without digital manipulation. For images shown here, gamma levels were adjusted in Adobe Photoshop CS3 (San Jose, CA). Identical gamma level adjustments were made for age-matched mutant and control images.

ISH

Sense and antisense riboprobes were generated against full-length *col19a1*, *syt 1*, and *syt2* IMAGE Clones (EMM1002-97504659 *[col19a1]*; MM1013-9199901 *[syt1]*; MMM1013-7512379 *[syt2]*; Open Biosystems, Huntsville, AL) or an 800-bp fragment of *parv* (corresponding to nucleotides 2–825) polymerase chain reaction (PCR)-cloned into pGEM Easy T vector (Promega, Madison, WI) with the following primers: 5′-TCT GCT CAT CCA AGT TGC AG-3′ and 5′-TCC TGA AGG ACT CAA CCC C-3′. Riboprobes were synthesized using digoxigenin (DIG) or fluorescein-labeled UTP (Roche, Mannheim, Germany) and the MAXI-Script In Vitro Transcription Kit (Ambion, Austin, TX). Probes were hydrolyzed to ≈ 500 nt. Coronal brain sections were prepared and hybridized at 65°C as previously described (Yamagata et al., 2002). Bound riboprobes were either detected by alkaline phosphatase (AP)-conjugated anti-DIG antibodies and colorimetric staining with the AP substrate NBT/BCIP (Roche), or detected by horseradish peroxidase (POD)-conjugated anti-DIG or anti-fluorescein antibodies and fluorescent staining with Tyramide Signal Amplification (TSA) systems (PerkinElmer, Shelton, CT). For double fluorescent in situ hybridization (D-FISH), after the first TSA reaction sections were washed with TBS, incubated with 0.3% H_2O_2 for 30 minutes, and reacted with the second POD-conjugated antibody. For fluorescent ISH coupled with immunohistochemistry (FISH-IHC) standard IHC was performed after completing the TSA amplification step described above. In some cases antibody-binding epitopes were destroyed during ISH, hampering IHC analysis. In such cases D-FISH was applied. However, most antibodies applied here were not hindered by ISH (see Supporting Fig. 1). Images were obtained on a Zeiss AxioImager A1 fluorescent microscope or a Leica SP2 scanning confocal microscope.

Western blot analysis

Mouse brains were perfused with PBS and hippocampal or cerebellar tissues were dissected in ice-cold PBS. Tissue was lysed in modified loading buffer containing 50 mmol/L Tris-HCl, pH 6.8, 2% sodium dodecyl sulfate (SDS), 10% glycerol, and protease inhibitors (1 mmol/L PMSF). Samples were homogenized, boiled for 10 minutes, centrifuged at 12,000*g* for 10 minutes, and insoluble material was removed. Protein concentrations were determined by bicinchoninic acid (BCA) protein assay (Pierce, Rockford, IL). Equal amounts of protein were loaded and separated by SDS-PAGE and transferred to PVDF membrane as described previously (Fox and Sanes, 2007). After blocking in 5% nonfat milk in PBS (containing 0.05% Tween20), PVDF membranes were incubated with appropriate primary antibodies, followed by HRP-conjugated secondary antibodies. Immunoblotted proteins were detected with enhanced chemiluminescent detection system (ECL Plus, Amersham Pharmacia Biotech, Piscataway, NJ) as previously described (Fox et al., 2003). Densitometry was performed using NIH ImageJ (Bethesda, MD).

Cresyl violet stain

Mouse brains were fixed in 4% PFA (in PBS) for 12 hours at 4°C, washed in PBS several times, sectioned on an Oxford vibratome (≈70 μm), collected on slides, and air-dried overnight. Dried sections were subsequently hydrated in 95%, 70% ethanol, and distilled water, stained with filtered cresyl violet solution (5 mg/mL cresyl violet acetate, 0.34 M acetic acid, 60 mM sodium acetate) for 1–3 minutes, rinsed in water, and subsequently dehydrated with 70%, 95%, and 100% ethanol. Slides were immersed in HistoClear (National Diagnostics, Atlanta, GA) for 10 minutes, air-dried, and were mounted with Permount. Images were acquired on an Olympus BX51 microscope with an Olympus OLY-750 color CCD camera.

Reverse Transcription-Polymerase Chain Reaction (RT-PCR)

RNA was isolated using the BioRad Total RNA Extraction from Fibrous and Fatty Tissue kit (BioRad, Hercules, CA). Concentrations of RNA samples were determined spectrophotometrically with a NanoDrop ND-1000 (Wilmington, DE). cDNAs were generated from 200 ng of RNA with the Superscript II Reverse Transcriptase First Strand cDNA Synthesis kit (Invitrogen, La Jolla, CA). For bench-top RT-PCR, the following *col19a1* primers were used: 5′-TTCTGT GGC AAC TGT CAA GC-3′; 5′-TTT CTC CCC GTG TAT TCC AG-3′. *Gapdh* primers were: 5′-AAC TTT GGC ATT GTG GAA GG-3′ and 5′-ACA CAT TGG GGG TAG GAA CA-3′. PCR products were amplified on an Eppendorf Mastercycler EP with the following cycling conditions: 94°C for 2 minutes, followed by 30 cycles of amplification (95°C for 15 seconds, 55°C for 30 seconds, 68°C for 60 seconds), and 2 minutes at 68°C. Products were visualized by separation on 2% agarose gels with 0.0001% ethidium bromide and images acquired with a FOTO-Dyne system (Fisher, Pittsburgh, PA). For quantifying mRNA levels, real-time quantitative RT-PCR (qPCR) was performed on a Chromo 4 Four-Color Real-time system (BioRad) using iQ SYBRGreen Supermix (BioRad). *Col19a1* primers for qPCR were 5′-ATT GGA CAT AAG GGC GAC AA-3′ and 5′-AGT CTC CTT TGG CTCCTG GT-3′. *Gapdh* primers for qPCR were 5′-CGTCCC GTA GAC AAA ATG GT-3′ and 5′-TTG ATG GCA ACA ATC TCC AC-3′. qPCR primers were designed over introns. The following cycling conditions were used with 20 ng of RNA: 95°C for 15 minutes, followed by 40 cycles of amplification (94°C for 15 seconds, 60°C for 20 seconds, 72°C for 20 seconds, read plate) and a melting curve analysis. Relative quantities of RNA were determined using the DDCT method (Livak and Schmittgen, 2001).

Immuno-electron microscopy (ImmunoEM)

Tissue was fixed in 4% PFA/ 1%glutaraldehyde in 0.125 M phosphate buffer (pH 7.4), sectioned on an Oxford vibratome (40–50 μm), and floating sections were stained with anti-Syt2 antibodies in IHC blocking buffer. Syt2 antibodies were detected with biotin-conjugated secondary antibodies (Vector Laboratories) followed by VectaStain ABC amplification (Vector) and 3,3′-diaminobenzidine (DAB) staining. ImmunoEM tissue was processed using standard procedures (Fox et al., 2004) in the Department of Anatomy and Neurobiology Microscopy Facility. Ultrathin sections were collected on 300 mesh Gilder thin bar grids (Electron Microscopy Sciences, Fort Washington, PA), stained with uranyl acetate and lead citrate, and imaged on a Jeol JEM-1230 transmission electron microscope equipped with a Gatan 4K × 4K CCD camera, interfaced with Digital micrograph software. Pseudo-coloring of EM micrographs performed in Adobe PhotoShop.

RESULTS

Col19a1, the gene encoding collagen XIX, is expressed by neurons in the mammalian hippocampus

To characterize the expression pattern of *col19a1* in the developing mouse brain, RT-PCR analysis was performed on RNA isolated from various regions of postnatal day 14 (P14) mouse brain. *Col19a1* mRNA was detected in hippocampus and cortex (Fig. 1B). To localize *col19a1* mRNA within the developing hippocampus, ISH was performed. At P14, hippocampal neurons, detected here with riboprobes directed against neuronally expressed *syt1* (which encodes the synaptic vesicle-associated protein synaptotagmin 1), are concentrated in stratum pyramidalis (of CA1-CA3 and subiculum) and in the granular layer of the dentate gyrus (DG) (Fig. 1C). These layers contain excitatory principle neurons (either pyradmidal neurons or granule cells) and sparsely distributed classes of interneurons. Other classes of *syt1*-expressing interneurons diffusely populate strata oriens, radiatum, and lacunosum-moleculare of CA1-3, the hilus of the DG, and the polymorphic and molecular

layers of the subiculum (Fig. 1C). In contrast to vast *syt1* expression, *col19a1* riboprobes labeled only a small population of hippocampal cells (Fig. 1D; sense controls shown in Fig. 1E). In the DG, *col19a1*-expressing cells were largely confined to the hilus (Fig. 1D). In CA regions, *col19a1* was most abundant in strata oriens, radiatum, and lacunosum-moleculare, although a few *col19a1*-expressing cells were also present in stratum pyramidalis (Fig. 1D'). In subiculum, *col19a1*-expressing cells more densely populated the stratum pyramidalis than in the flanking molecular and polymorphic layers (Fig. 1D, Fig. 2A). ISH also confirmed *col19a1* mRNA expression in cortex and demonstrated its absence in other regions of P14 mouse brain (Fig. 1D).

We next sought to determine the identity of hippocampal cells expressing *col19a1* mRNA. To accomplish this we combined localizing *col19a1* mRNA with mRNAs or proteins expressed by major subtypes of hippocampal cells, i.e., neurons, astrocytes, oligodendrocytes, microglia, and endothelial cells. Double fluorescent ISH (D-FISH) revealed widespread coexpression of *syt1* mRNA in *col19a1*-expressing cells (Fig. 2A,B). Thus, neurons express *col19a1*, which was confirmed by immunolabeling with the neuronal marker NeuN (Fig. 2C). The sparse distribution of *col19a1* mRNA (Fig. 1D, Fig. 2A) suggested interneurons may express *col19a1*. Indeed, *col19a1* mRNA was present in cells containing the interneuron-specific enzyme glutamate decarboxylase 67 (Gad67) (Fig. 2D).

While these data demonstrate interneuronal expression of *col19a1*, they do not rule out its expression by nonneuronal cells. Coupling fluorescent ISH with IHC (FISH-IHC) for GFAP (which labels astrocytes) and Iba-1 (which labels microglia) revealed no coexpression in *col19a1*-expressing cells (Fig. 2E,F). Thus, hippocampal *col19a1* mRNA expression appears restricted to interneurons.

Developmental regulation of *col19a1* in the hippocampus

Dynamic spatiotemporal expression patterns of several synaptic organizing molecules correlate with synaptogenesis (e.g., Lucas and Salinas, 1997; Hall et al., 2000; Umemori et al., 2004; Fox et al., 2007). Therefore, we examined the developmental regulation of hippocampal *col19a1* mRNA by qPCR. The highest levels of *col19a1* mRNA were present at birth (P0) and after the first postnatal week (P7; Fig. 3A). Significantly reduced *col19a1* mRNA levels were observed by P14, after which time no significant changes in expression were observed (Fig. 3A).

Developmental regulation of hippocampal *col19a1* was further assessed by FISH. As opposed to global quantities of *col19a1* mRNA measured by qPCR, FISH revealed relative numbers of *col19a1*-expressing neurons. Since hippocampal size and shape vary greatly based on rostral-caudal location, numbers of *col19a1*-expressing neurons were obtained only from sections containing both ventral and dorsal lateral geniculate nuclei (vLGN and dLGN), delineated by calbindin (Calb) immunostaining (Luth et al., 1993; for example, see Fig. 8A). Similar to qPCR results, significantly higher numbers of *col19a1*-expressing neurons were present during the first postnatal week of development than in adults (Fig. 3B–E). Numbers of *col19a1*-expressing neurons in P14 hippocampi were also significantly higher than in adult tissue (Fig. 3B). In P14 hippocampi, *col19a1* riboprobes reactivity appeared reduced in subsets of cells, suggesting these cells had begun to downregulate *col19a1* (Fig. 3F,G). This likely explains the difference between levels of *col19a1* measured by qPCR and ISH at P14. Taken together, these results demonstrate that the highest levels of *col19a1* mRNA occur in the first 2 postnatal weeks coinciding with the peak of synaptogenesis (Vaughn, 1989). Interestingly, these spatiotemporal expression patterns were specific to hippocampus as levels of cortical *col19a1* mRNA continue to increase with age (Sumiyoshi et al., 1997, 2001).

Importantly, developmental changes in the relative numbers of *col19a1*-expressing neurons were not similar in all regions of the hippocampus. In CA fields and the hilus of the DG, many *col19a1*-expressing neurons persisted into adulthood (Fig. 3C–E). However, in subiculum, which exhibited the highest density of *col19a1*-expressing neurons at P7 (see arrowheads in Fig. 2A), few *col19a1*-expressing neurons were present in adult tissue (Fig. 3H). In fact, in subiculum both the number of positive neurons and intensity of mRNA labeling were dramatically reduced by P14 (Fig. 3G). Based on both distribution and developmental regulation, these data suggest that multiple classes of interneurons express *col19a1* mRNA.

Distinct populations of hippocampal interneurons express *col19a1*

The rodent hippocampus is rich in neuronal diversity (reviewed in Klausberger and Somogyi, 2008; Danglot et al., 2006; McBain and Fisahn, 2001). Although hippocampal interneurons are classified based on multiple criteria (i.e., morphology, electrophysiology, or expression of neurochemicals), only one approach was compatible with our method to localize *col19a1* mRNA–immunolabeling for subclass-specific neurochemicals. Three such neurochemicals, NPY, Som, and Calb, were present in *col19a1*-positive neurons (Fig. 4A–D). Antibodies or riboprobes directed against other interneuron-specific neurochemicals, such as Calr or *parv* (the gene encoding parvalbumin) showed no coexpression with *col19a1* mRNA (Fig. 4E,F).

On the basis that *col19a1*-expressing neurons contain NPY, Som, or Calb, we asked whether these neurochemicals could distinguish the different populations of *col19a1*-expressing neurons described above. To this end, we examined coexpression of *col19a1* mRNA with NPY, Som, or Calb in each region of the hippocampus.

NPY-immunoreactive interneurons—A large majority of *col19a1*-expressing neurons in CA1, CA3, and the hilus contained NPY (Fig. 5A–C). In CA regions, NPY-*col19a1* coexpressing neurons were found in all strata (for example, see Fig. 5B). In subiculum, few (if any) NPY-immunoreactive cells contained *col19a1* mRNA (Fig. 5D).

Som-immunoreactive interneurons—Many Som-immunoreactive interneurons in CA1, CA3, and the hilus contained *col19a1* mRNA (Fig. 6A–D). However, two main differences were noted between NPY-*col19a1* and Som-*col19a1* cells. First, in CA1 and CA3 Som-*col19a1* coexpressing neurons were confined to stratum oriens (Fig. 6A–C). No Som-*col19a1* coexpressing neurons were observed in strata pyramidalis, radiatum, or lacunosum-moleculare of CA1 or CA3. Second, approximately half of the subicular *col19a1*-expressing neurons contained Som (Fig. 6E).

Calb-immunoreactive interneurons—Only a small subset of *col19a1*-expressing neurons contained Calb in CA1 and CA3 (Fig. 7A,B; see also Fig. 3C–E). These Calb-*col19a1*-expressing cells were randomly distributed throughout strata oriens, radiatum, and lacunosum-moleculare. Coexpression of *col19a1* mRNA and Calb was even less frequently observed in the hilus (Fig. 7C). In the developing subiculum, however, approximately half of the *col19a1*-expressing neurons contained Calb (Fig. 7D).

Collagen XIX is required for normal nerve terminal formation in subiculum

Since nonfibrillar collagens direct peripheral nervous system (PNS) synaptogenesis in both vertebrates and invertebrates (Ackley et al., 2003; Fox et al., 2007; Fox, 2008), we next asked whether CNS-derived collagen XIX was necessary for the formation of hippocampal synapses in previously generated collagen XIX-deficient mouse mutants (Sumiyoshi et al., 2004). *Col19a1*$^{-/-}$ mutants are smaller than littermate controls and most die by weaning,

both presumably due to defects in esophageal muscle physiology and morphology (Sumiyoshi et al., 2004). Here, cresyl violet staining revealed few differences between mutant and control brains besides a reduction in size in the absence of collagen XIX (Fig. 8). Size differences were not specific to hippocampus or cortex but were seen in all CNS regions (e.g., see dorsal lateral geniculate nuclei [dLGN] in Fig. 8). Besides being smaller, the morphological organization of mutant hippocampi appeared strikingly normal in the absence of collagen XIX (Fig. 8). Thus, collagen XIX was dispensable for the gross organization of the mammalian hippocampus.

To assess nerve terminal formation in the absence of collagen XIX, immunolabeling of synaptic vesicle-associated proteins–hallmark components of presynaptic terminals–was performed on mutant and control hippocampi. We focused on subiculum since the density of *col19a1*-expressing neurons was highest in this region during synaptogenesis. While the expression and distribution of many synaptic vesicle-associated proteins was unchanged in mutant subiculum, the expression and distribution of synaptotagmin 2 (Syt2) was markedly altered in mutants (Fig. 9, Fig. 10).

Syt2 is a member of the large synaptotagmin family of vesicle-associated proteins previously shown to be present in synapses within stratum pyramidalis of CA1-3 (Wendland et al., 1991; Ullrich et al., 1994; Südhof, 2002; Fox and Sanes, 2007). After the first postnatal week of development Syt2 appeared largely concentrated in both stratum pyramidalis of CA2 and the adjacent portion of CA3 and in the pyramidal and polymorphic layers of subiculum (Fig. 9A; see Fig. 8C for subicular layers). Sparse Syt2-containing nerve terminals were also observed in strata oriens, radiatum and lacunosum-moleculare at this age (Fig. 9D). By the end of the third postnatal week, the distribution of Syt2-containing nerve terminals expanded to include stratum pyramidalis of all CA regions and appeared similar to its adult distribution (Wendland et al., 1991; Ullrich et al., 1994; Fox and Sanes, 2007). In collagen XIX-deficient mutants, a striking reduction in Syt2-immunostaining levels was observed in subiculum (Fig. 9E,F; see arrows). A less obvious, but equally significant, reduction in Syt2-immunoreactive nerve terminals was observed in strata oriens, radiatum, and lacunosum-moleculare of CA1-3 regions (Fig. 9H). Reduced levels of Syt2 were specific to subiculum and these sparsely distributed terminals; Syt2-immunoreactivity appeared similar to controls in mutant stratum pyramidalis of all CA regions (Fig. 9A,B; see arrowhead).

Reduced levels of hippocampal Syt2, but not other syn-aptic vesicle-associated proteins or presynaptic machinery, were confirmed and quantified by Western blot analysis (Fig. 10A,B). Quantities of Syt2 were significantly lower in mutant hippocampi in all ages examined; however, differences between mutant and control samples decreased with age. While this may suggest a compensatory mechanism assembles Syt2-positive nerve terminals in the absence of collagen XIX, it more likely reflects development of Syt2-containing terminals in CA1 and CA3 stratum py-ramidalis that do not require collagen XIX. Reduced levels of Syt2 were specific to mutant hippocampus as collagen XIX-deficient cerebella contained normal levels of Syt2 (Fig. 10A,B). Furthermore, the altered distribution and reduced levels of Syt2 in mutant hippocampi were not due to cell-autonomous defects in cells that normally express *col19a1* mRNA since *col19a1* and *syt2* were largely expressed by different subsets of hippocampal interneurons (Fig. 11).

To identify whether collagen XIX was necessary for excitatory or inhibitory synapses, we sought to determine the type of subicular synapses containing Syt2. IHC with antibodies directed against both isoforms of Gad (Gad65/67) demonstrated that most Syt2-containing nerve terminals in the mouse subiculum were inhibitory (Fig. 12A–C). A large percentage of these Gad/Syt2-containing nerve terminals resembled axo-somatic synapses (see white

arrowheads in Fig. 12A–C), although terminals not associated with cell somas also coexpressed Syt2 and Gad65/67 (see white arrows in Fig. 12A). Ultrastructural analysis of P10 wildtype subiculum confirmed the presence of Syt2 in at least axo-somatic synapses (Fig. 12D). While these analyses do not rule out Syt2 expression in excitatory terminals (see green arrows in Fig. 12A), they demonstrate that the vast majority of Syt2-containing subicular synapses are inhibitory.

To assess whether inhibitory synapses were malformed in the absence of collagen XIX we examined Gad67 distribution in mutant subiculum by IHC. In stratum pyramidalis of subiculum (where Syt2-immunoreactivity is concentrated in controls [Fig. 9a]) two notable differences in Gad67 distribution were observed in mutants. First, levels of Gad67 were higher in cell bodies and their processes in mutants than in controls (see arrows and arrowheads in Fig. 12F). Second, whereas a punctate synaptic distribution of Gad67 was apparent in controls, Gad67-immunoreactivity in mutants appeared diffuse (Fig. 12E,E',F,F'). Differences in Gad67 distribution were specific to stratum pyramidalis, as Gad67 distribution in the molecular layer of mutant subiculum resembled that of controls (Fig. 12E,E",F,F"). In addition to differences in Gad67 distribution, abnormal levels of gephyrin, a postsynaptic scaffolding molecule present only at inhibitory synapses (Cabot et al., 1995;Craig et al., 1996), were observed in mutant hippocampal extracts. Surprisingly, however, levels of gephyrin were significantly elevated in mutants (Fig. 12G,H). Levels of postsynaptic density 95 (PSD-95), a postsynaptic scaffolding component present at excitatory synapses (Hunt et al., 1996;El-Husseini et al., 2000), were indistinguishable between mutants and controls (Fig. 12G). Taken together, these data suggest collagen XIX is required for the organization of inhibitory subicular synapses.

DISCUSSION

Many families of ECM molecules known to direct synapse formation at the NMJ also regulate CNS synaptogenesis. Agrin contributes to the organization and function of central synapses and dendritic spines, perhaps through interactions with transmembrane α3 Na^+/K^+ ATPase (Ferreira, 1999; Bose et al., 2000; Tournell et al., 2006; Hilgenberg et al., 2006; Reif et al., 2007; Ksiazek et al., 2007; Matsumoto-Miyai et al., 2009). Laminin heterotrimers containing β2 chains are present in central synaptic clefts and are necessary for synaptic organization in both retina and hippocampus (Libby et al., 1999; Egles et al., 2007). The results presented here suggest that a third family of NMJ-organizing matrix molecules, nonfibrillar collagens, are expressed by neurons and contribute to central synaptogenesis. Specifically, several classes of hippocampal interneurons express *col19a1*, which is necessary for the normal organization of subsets of Syt2-containing hippocampal nerve terminals. Thus, these studies not only advance our understanding of subicular synaptogenesis but they challenge the preexisting notion that collagens are absent from and do not contribute to the development of the mammalian brain.

Subclasses of hippocampal interneurons express *col19a1* mRNA

The complexity of interneuronal diversity is staggering. In CA1 alone, at least 21 subclasses of interneurons have been identified (Klausberger and Somogyi, 2008) based on the expression of distinct neurochemical markers (e.g., Calb, Calr, Som, NPY, Parv; Freund and Buzsaki, 1996; McBain and Fisahn, 2001; Danglot et al., 2006), action potential firing patterns (Lacaille et al., 1987; Kawaguchi and Hama, 1988), response to neuromodulators (Parra et al., 1998), and neuronal or synaptic morphology (Ramon y Cajal, 1911; Freund and Buzsaki, 1996; McBain and Fisahn, 2001; Danglot et al., 2006; Klausberger and Somogyi, 2008). Here we sought to identify the types of interneurons that express *col19a1* mRNA

based on coexpression of neurochemical markers. For a summary of these results, see Table 2.

We will focus our discussion here on classes of interneurons in CA regions, where interneuron diversity has been best characterized (Danglot et al., 2006; Klausberger and Somogyi, 2008). While we set out to identify classes of interneurons expressing *col19a1*, we were more successful in identifying classes of interneurons that do not generate *col19a1*. The sparsity of *col19a1* mRNA within stratum pyramidalis (Fig. 1D, Fig. 2A, Fig. 3C–E), and lack of expression in parvalbumin containing neurons (Fig. 4F), suggest basket and chandelier (or axo-axonic) cells do not express *col19a1* mRNA (Howard et al., 2005; Danglot et al., 2006; Klausberger and Somogyi, 2008). The absence of *col19a1* mRNA in Calr-immunoreactive interneurons (Fig. 4E) further ruled out *col19a1* expression in several classes of interneuron-specific interneurons (IS-1 and IS-3) (Gulyas et al., 1996; Freund and Gulyas, 1997). It remains unclear whether the third subclass of interneuronselective interneurons, which lack Calr but contain vaso-active intestinal peptide (VIP) (Acsády et al., 1996a,b; Freund and Gulyas, 1997) express *col19a1* mRNA. Lastly, our finding that *col19a1*-expressing cells in strata radiatum and lacunosum-moleculare do not contain Som (Fig. 6) revealed many stratum lacunosum-moleculare projecting interneurons, such as LM, R-LM, and P-LM cells, lack *col19a1* (Oliva et al., 2000; Danglot et al., 2006).

Identifying specific classes of interneurons that express collagen XIX proved more difficult due to the wide distribution of *col19a1* mRNA and only partial overlap with either NPY-, Som-, or Calb-immunoreactive cells (Figs. 3C–E, 4A–D, 5–7). In stratum oriens, however, it was evident that one well-characterized class of interneurons contained *col19a1* mRNA: stratum orienslacunosum-moleculare (O-LM) cells. O-LM cells, whose somas lie in stratum oriens and axons project to stratum lacunosum-moleculare, contain both NPY and Som (Ko¨hler et al., 1987; Freund and Buzaki, 1996; Danglot et al., 2006). The high degree of overlap of *col19a1* mRNA with either Som- or NPY-immunoreactivity in stratum oriens (Fig. 5, Fig. 6) strongly suggests that O-LM cells generate collagen XIX.

Except for O-LM cells, definitive identification of *col19a1*-expressing cells remains unresolved. Outside of stratum oriens, NPY-immunoreactive *col19a1*-expressing neurons likely belong to neurogliaform, ivy cell, or bistratified subclasses of interneurons, based on both location and the absence of Parv, Calr, or Som (Markram et al., 2004; Price et al., 2005; Fuentealba et al., 2008). While Calb-immunoreactivity is associated with several widely distributed classes of interneurons, including bistratified cells, Schaffer collateral-associated cells, horizontal trilaminar cells, radial trilaminar cells, Calb-Calr coexpressing cells, and hippocampal-septal projecting cells (Sik et al., 1995; Cope et al., 2002; Markram et al., 2004; Danglot et al., 2006), the sparse, random distribution of Calb-*col19a1* coexpressing cells make it unclear what class of interneurons these belong to. It is noteworthy that a class of CA1 pyramidal neurons also express Calb (Rami et al., 1992; Molinari et al., 1996; Klausberger and Somogyi, 2008); however, the distribution and morphology of Calb-*col19a1* coexpressing cells rule out the possibility that pyramidal neurons express *col19a1* mRNA (Fig. 3D,E).

It is also difficult from these analyses to accurately conclude what cell types express *col19a1* in other regions of the hippocampus. In subiculum, where *col19a1* expression is more concentrated and developmentally regulated (Fig. 2A, Fig. 3F–H), less is known about numbers or types of interneurons. Assuming similar classes of interneurons exist in subiculum (for example, see Knopp et al., 2008), our studies suggest that different subsets of interneurons express *col19a1* in subiculum than in CA regions. Not only do *col19a1*-expressing O-LM cells not exist in subiculum, but few, if any, NPY-containing interneurons express *col19a1* mRNA in this region (Fig. 5–Fig. 7). Furthermore, in subiculum a greater

ratio of Calb-containing interneurons express *col19a1* mRNA and the distribution of Som-*col19a1* coex-pressing cells is far less restricted (Fig. 6, Fig. 7).

Despite spatial, temporal, and neurochemical diversity, *col19a1*-expressing cells may share one commonality–they may be derived from a single neurogenic region. Hippocampal interneurons are derived from two neurogenic regions during embryogenesis–the medial ganglionic eminence (MGE) and the caudal ganglionic eminence (CGE) (Pleasure et al., 2000; Nery et al., 2002). Fate mapping has shown Som-immunoreactive interneurons arise from the MGE (Wichterle et al., 2001). Mice lacking the Nkx2.1 homeobox gene, which exhibit malformed MGEs, fail to generate NPY-, Som-, and a large set of Calb-containing interneurons (Pleasure et al., 2000). Furthermore, in vitro cultures generated from these Nkx2.1 mutants generate Calr-immunoreactive interneurons but not Parv-, Som-, or NPY-containing interneurons (Xu et al., 2004). Comparing these data with our studies led us to speculate that *col19a1*-expressing interneurons may arise solely from MGE. Generation from the MGE alone, however, does not predetermine whether a neuron expresses *col19a1* since Parv-immunoreactive cells are also born from MGE progenitors.

Collagen XIX is required for synapse formation in subiculum

Cell-type-specific expression and differential regulation suggest collagen XIX might have multiple functions in the mammalian hippocampus. However, collagen XIX appears largely dispensable for the gross organization of the mammalian hippocampus (Fig. 8). Distribution and expression of several cell-type-specific markers, axonal markers, and synaptic markers appear normal in the absence of collagen XIX (Fig. 9–Fig. 11). Furthermore, both the distribution and morphology of interneurons that normally express *col19a1*, such as Calb-immunoreactive subicular neurons, appear normal in the absence of collagen XIX (Fig. 9F'). Together, these analyses further confirm that much of hip-pocampal development proceeds normally in the absence of collagen XIX. However, the altered distribution of presynaptic Syt2 in mutants lacking collagen XIX (Fig. 9A,B-,D,E,F,H,I) suggests that collagen XIX is necessary for the normal organization of subsets of hippocampal nerve terminals. Interestingly, while these studies demonstrate an essential role of collagen XIX in synaptic organization, previous studies implicated this collagen in neuromuscular function in the PNS. Specifically, NO-dependent relaxation following contractions in lower esophageal sphincter muscle requires the presence of a collagen XIX-rich basal lamina. Although it remains unclear whether pre- and postsynaptic partners are malformed at esophageal sphincter synapses in collagen XIX-deficient mutants, it is likely that the absence of this collagen results in a disorganized syn-aptic basal lamina (Myers et al., 1997,2003;Sumiyoshi et al., 2004). Together with studies presented here, this suggests that collagen XIX contributes to synaptic organization and/or function at multiple anatomical locations.

The presence of Syt2 in inhibitory synapses throughout neocortex, hippocampus, brainstem, and cerebellum (Ullrich et al., 1994; Marquez et al., 1995; Pang et al., 2006a,b; Fox and Sanes, 2007) raised the possibility that collagen XIX is required for the formation of some inhibitory hippocampal nerve terminals. Indeed, IHC and ultrastructural analysis confirmed that Syt2 was present at inhibitory synapses (Fig. 12A–D). Altered distribution of Gad67 and abnormal levels of gephyrin in mutants (Fig. 12) suggest that inhibitory synapses require collagen XIX. Interestingly, mutant levels of gephyrin were increased in contrast to reduced levels of Syt2 (Fig. 10, Fig. 12G,H). Similar mismatched levels of pre- and postsynaptic components have been reported in other mutant mice exhibiting hippocampal synaptic defects (e.g., Rodena-Ruano et al., 2006). Several explanations for this mismatch are possible. Postsynaptic neurons might compensate for defective or reduced quantities of nerve terminals (and any transsynaptic organizing cues that they might generate) by increasing postsynaptic apparati size. Similar compensatory mechanisms have been well

documented for other types of intercellular signaling in the CNS (e.g., Rice et al., 1998). Alternatively, defects in inhibitory synapses in collagen XIX-deficient mutants may result in reduced inhibitory activity. As increased levels of synaptic activity speed the rate of postsynaptic density component turnover (Ehlers, 2003), decreased levels of inhibitory activity may slow gephyrin turnover in mutant hippocampi. Of course, it is also possible that increased levels of gephyrin are not directly linked to the altered distributions of Gad67 and Syt2 in collagen XIX-deficient mice.

Mechanisms for collagen XIX in subicular synapse formation

Col19a1 and *syt2* are both expressed by hippocampal interneurons. However, it is unlikely that defects in collagen XIX-deficient hippocampi arise cell-autonomously. Complementary expression patterns and the observation that Syt1 and Syt2 are present in distinct sets of central synapses suggest that mammalian neurons typically express either *syt1* or *syt2* (Ullrich et al., 1994; Marqueze et al., 1995; Berton et al., 1997; Pang et al., 2006a,b; Fox and Sanes, 2007; Mittelsteadt et al., 2009). Our data demonstrate that *col19a1* mRNA is present in *syt1*-expressing cells and is present in very few syt2-expressing cells (Fig. 2A,B). These results are supported by previous reports documenting spatial and temporal expression patterns of *syt2* in the rodent hippocampus that differ from those described here for *col19a1* (Berton et al., 1997; Mittelsteadt et al., 2009). As such, we postulate that synaptic defects in collagen XIX-deficient mutants likely arise largely through non-cell-autonomous mechanisms. At present the exact nature of these mechanisms remains unclear.

One possibility is that synaptic defects in collagen XIX mutants are secondary to alterations in other aspects of hippocampal development such as cell specification, migration, or differentiation. Our analysis, however, failed to identify any striking defects in number, position, or morphology of either excitatory or inhibitory neurons in mutant hippocampi (Fig. 8, Fig. 9A,B’,E,F’). Moreover, the synaptic defects reported here do not reflect a general delay in development in the absence of collagen XIX since many aspects of hippocampal development proceeded normally in mutants: Calb-immunoreactive interneurons appear normally differentiated in collagen XIX mutants (Fig. 9A,B’,E,F’); granular cell-derived mossy fibers targeted and innervated stratum lucidum of CA3 at similar times in mutants and controls (Fig. 9A,E); quantities of developmentally regulated synaptic machinery components, such as synapsin (Melloni et al., 1993;Melloni and Degennaro, 1994), PSD-95 (Chang et al., 2009), vesicular glutamate transporter 1 (VGlut1) and VGlut2 (Kaneko et al., 2002), appeared normal in mutant hippocampi (Fig. 10A, Fig. 12G); Syt2-containing presynaptic terminals in stratum pyramidalis of CA1-3 developed normally in the absence of collagen XIX (Fig. 9G).

Alternatively, collagen XIX might act indirectly at synapses by altering the expression or distribution of other synaptic organizers. Although few studies have examined cues that induce synapse formation in subiculum, several factors capable of directing synaptogenesis elsewhere in hippocampus have been identified. Neurons in CA subfields express an array of synaptic organizing factors, including SynCAMs (Fogel et al., 2007; Thomas et al., 2008), neuroligins (Song et al., 1999), neurexins (Ullrich et al., 1995), ephrins and Eph receptors (for review, see Martinez and Soriano, 2005), Wnts (Salinas and Zou, 2008; Davis et al., 2008), cadherins (Benson and Tanaka, 1998; Togashi et al., 2002; Bekirov et al., 2008), FGFs and FGF receptors (Kuzis et al., 1995; Li et al., 2002), agrin (O’Connor et al., 1994; Cohen et al., 1997; Lesuisse et al., 2000), and laminins (Egles et al., 2007). It remains unclear whether collagen XIX can bind or modulate the expression of any of these organizing molecules. Likely collagen XIX-interacting candidates are synaptogenic FGFs (FGF2, FGF7, FGF10, FGF22) (Li et al., 2002; Umemori et al., 2004; Fox et al., 2007), which could potentially complex with collagen XIX via their mutual ability to bind heparin

(Jang et al., 1997; Igarashi et al., 1998; Myers et al., 2003). However, synaptic defects reported to date in mutants lacking synaptogenic FGFs or their receptors do not resemble those reported here for collagen XIX (Umemori et al., 2004; Terauchi et al., 2008). In fact, synaptic defects reported in many of the previously characterized synaptic organizing molecules result in different phenotypes than those described here in the absence of collagen XIX (e.g., Missler et al., 2003; Henkemeyer et al., 2003; Egles et al., 2007; Ksiazek et al., 2007; Chubykin et al., 2007; Tabuchi et al., 2007; Xu and Henkemeyer, 2009).

A third possibility is that collagen XIX may act directly at synapses by binding and activating a transmembrane receptor. Collagenous sequences (hallmark features of both fibrillar and nonfibrillar collagens) are known to bind integrins, discoidin domain receptor tyrosine kinases (DDR1 and DDR2), and leukocyte-associated immunoglobulin-like receptor 1 (LAIR-1) (Vogel et al., 1997; Abdulhussein et al., 2004; Lebbink et al., 2006) several of which are present in the mammalian CNS (Pinkstaff et al., 1999; Bhatt et al., 2000). While little is known about the roles of DDRs and LAIR-1 in neural development (but see Bhatt et al., 2000), integrins contribute to axonal growth, dendritic development, synaptogenesis, synaptic plasticity, and synaptic function (e.g., DeFreitas et al., 1995; Chavis and Westbrook, 2001; Chun et al., 2001; Pasterkamp et al., 2003; Chan et al., 2003, [2006], 2007; Huang et al., 2006; Shi and Ethell, 2006; Webb et al., 2007). In addition to activating collagenous receptors, noncollagenous (NC) domains of nonfibrillar collagens can act as signaling molecules after being proteolytically released (Ortega and Werb, 2002; Kalluri, 2003). In the PNS, cleaved collagen IV NC domains induce motor nerve terminal differentiation (Fox et al., 2007; Fox, 2008). Since collagen XIX NC domains share similar functions to those of collagen IV outside of the nervous system (Kalluri, 2003; Ramont et al., 2007), they may be capable of inducing presynaptic differentiation in hippocampal neurons. Receptors for NC domains also include integrins, albeit a different set of integrins than those capable of binding collagenous sequences. These include α3β1, α5β1, αvβ3, and αvβ5 integrins (Kalluri, 2003; Pedchenko et al., 2004; Borza et al., 2006), several of which are not only expressed by hippocampal neurons but are present at synaptic sites (Pinkstaff et al., 1999; Chan et al., 2003, 2007; Huang et al., 2006; Werb et al., 2007).

Supplementary Material

Refer to Web version on PubMed Central for supplementary material.

Acknowledgments

We thank A.R. McQuiston, H. Umemori, B. Fuss, J.T. Povlishock, and S. Henderson for helpful discussions regarding the article, experimental design, and microscopy. Microscopy was performed at the VCU Department of Anatomy and Neurobiology Microscopy Facility supported, in part, with funding from NIH-NINDS Center Core grant (5P30NS047463-02). The monoclonal antibodies VGlut1 and VGlut2 were developed by and/or obtained from the UC Davis/NIH NeuroMab Facility, supported by NIH grant U24NS050606 and maintained by the Department of Neurobiology, Physiology and Behavior, College of Biological Sciences, University of California, Davis, CA.

Grant sponsor: National Institutes of Health (NIH); Grant number: AR38648 (to F.R.); Grant sponsor: A.D. Williams grant (to M.F.).

LITERATURE CITED

Abdulhussein R, McFadden C, Fuentes-Prior P, Vogel WF. Exploring the collagen-binding site of the DDR1 tyrosine kinase receptor. J Biol Chem 2004;279:31462–31470. [PubMed: 15136580]

Ackley BD, Kang SH, Crew JR, Suh C, Jin Y, Kramer JM. The basement membrane components nidogen and type XVIII collagen regulate organization of neuromuscular junctions in Caenorhabditis elegans. J Neurosci 2003;23:3577–3587. [PubMed: 12736328]

Acosta ML, Bumsted O'Brien KM, Tan SS, Kalloniatis M. Emergence of cellular markers and functional ionotropic glutamate receptors on tangentially dispersed cells in the developing mouse retina. J Comp Neurol 2008;506:506–523. [PubMed: 18041773]

Acsády L, Gorcs TJ, Freund TF. Different populations of vasoactive intestinal polypeptide-immunoreactive interneurons are specialized to control pyramidal cells or interneurons in the hippocampus. Neuroscience 1996a;73:317–334.

Acsády L, Arabadzisz D, Freund TF. Correlated morphological and neurochemical features identify different subsets of vasoactive intestinal polypeptide-immunoreactive interneurons in rat hippocampus. Neuroscience 1996b;73:299–315.

Arimura A, Sato H, Coy DH, Schally AV. Radioimmunoassay for GH-release inhibiting hormone. Proc Soc Exp Biol Med 1975;148:784–789. [PubMed: 1129301]

Armstrong JN, Saganich MJ, Xu NJ, Henkemeyer M, Heinemann SF, Contractor A. B-ephrin reverse signaling is required for NMDA-independent long-term potentiation of mossy fibers in the hippocampus. J Neurosci 2006;26:3474–3481. [PubMed: 16571754]

Bekirov IH, Nagy V, Svoronos A, Huntley GW, Benson DL. Cadherin-8 and N-cadherin differentially regulate pre- and postsynaptic development of the hippocampal mossy fiber pathway. Hippocampus 2008;18:349–363. [PubMed: 18064706]

Belenky MA, Yarom Y, Pickard GE. Heterogeneous expression of gamma-aminobutyric acid and gamma-aminobutyric acid-associated receptors and transporters in the rat suprachiasmatic nucleus. J Comp Neurol 2008;506:708–732. [PubMed: 18067149]

Benson DL, Tanaka H. N-cadherin redistribution during synaptogenesis in hippocampal neurons. J Neurosci 1998;18:6892–6904. [PubMed: 9712659]

Berton F, Iborra C, Boudier JA, Seagar MJ, Marqueze B. Developmental regulation of synaptotagmin I, II, III, and IV mRNAs in the rat CNS. J Neurosci 1997;17:1206–1216. [PubMed: 9006966]

Bhatt RS, Tomoda T, Fang Y, Hatten ME. Discoidin domain receptor 1 functions in axon extension of cerebellar granule neurons. Genes Dev 2000;14:2216–2228. [PubMed: 10970885]

Bjartmar L, Huberman AD, Ullian EM, Renteria RC, Liu X, Xu W, Prezioso J, Susman MW, Stellwagen D, Stokes CC, Cho R, Worley P, Malenka RC, Ball S, Peachey NS, Copenhagen D, Chapman B, Nakamoto M, Barres BA, Perin MS. Neuronal pentraxins mediate synaptic refinement in the developing visual system. J Neurosci 2006;26:6269–6281. [PubMed: 16763034]

Borza CM, Pozzi A, Borza DB, Pedchenko V, Hellmark T, Hudson BG, Zent R. Integrin alpha3beta1, a novel receptor for alpha3(IV) noncollagenous domain and a trans-dominant Inhibitor for integrin alphavbeta3. J Biol Chem 2006;281:20932–20939. [PubMed: 16731529]

Bose CM, Qiu D, Bergamaschi A, Gravante B, Bossi M, Villa A, Rupp F, Malgaroli A. Agrin controls synaptic differentiation in hippocampal neurons. J Neurosci 2000;20:9086–9095. [PubMed: 11124985]

Burden SJ, Sargent PB, McMahan UJ. Acetylcholine receptors in regenerating muscle accumulate at original synaptic sites in the absence of the nerve. J Cell Biol 1979;82:412–425. [PubMed: 479308]

Burgess RW, Nguyen QT, Son YJ, Lichtman JW, Sanes JR. Alternatively spliced isoforms of nerve- and muscle-derived agrin: their roles at the neuromuscular junction. Neuron 1999;23:33–44. [PubMed: 10402191]

Cabot JB, Bushnell A, Alessi V, Mendell NR. Postsynaptic gephyrin immunoreactivity exhibits a nearly one-to-one correspondence with gamma-aminobutyric acid-like immunogoldlabeled synaptic inputs to sympathetic preganglionic neurons. J Comp Neurol 1995;356:418–432. [PubMed: 7642803]

Chan CS, Weeber EJ, Kurup S, Sweatt JD, Davis RL. Integrin requirement for hippocampal synaptic plasticity and spatial memory. J Neurosci 2003;23:7107–7116. [PubMed: 12904471]

Chan CS, Weeber EJ, Zong L, Fuchs E, Sweatt JD, Davis RL. Beta 1-integrins are required for hippocampal AMPA receptor-dependent synaptic transmission, synaptic plasticity, and working memory. J Neurosci 2006;26:223–232. [PubMed: 16399691]

Chan CS, Levenson JM, Mukhopadhyay PS, Zong L, Bradley A, Sweatt JD, Davis RL. Alpha3-integrins are required for hippocampal long-term potentiation and working memory. Learn Mem 2007;14:606–615. [PubMed: 17848500]

Chang LR, Liu JP, Zhang N, Wang YJ, Gao XL, Wu Y. Different expression of NR2B and PSD-95 in rat hippocampal subregions during postnatal development. Microsc Res Tech 2009;72:517–524. [PubMed: 19306263]

Chavis P, Westbrook G. Integrins mediate functional pre-and postsynaptic maturation at a hippocampal synapse. Nature 2001;411:317–321. [PubMed: 11357135]

Christopherson KS, Ullian EM, Stokes CC, Mullowney CE, Hell JW, Agah A, Lawler J, Mosher DF, Bornstein P, Barres BA. Thrombospondins are astrocyte-secreted proteins that promote CNS synaptogenesis. Cell 2005;120:421–433. [PubMed: 15707899]

Chubykin AA, Atasoy D, Etherton MR, Brose N, Kavalali ET, Gibson JR, Südhof TC. Activity-dependent validation of excitatory versus inhibitory synapses by neuroligin-1 versus neuroligin-2. Neuron 2007;54:919–931. [PubMed: 17582332]

Chun D, Gall CM, Bi X, Lynch G. Evidence that integrins contribute to multiple stages in the consolidation of long term potentiation in rat hippocampus. Neuroscience 2001;105:815–829. [PubMed: 11530220]

Claudepierre T, Manglapus MK, Marengi N, Radner S, Champliaud MF, Tasanen K, Bruckner-Tuderman L, Hunter DD, Brunken WJ. Collagen XVII and BPAG1 expression in the retina: evidence for an anchoring complex in the central nervous system. J Comp Neurol 2005;487:190–203. [PubMed: 15880472]

Cohen NA, Kaufmann WE, Worley PF, Rupp F. Expression of agrin in the developing and adult rat brain. Neuroscience 1997;76:581–596. [PubMed: 9015340]

Cope DW, Maccaferri G, Marton LF, Roberts JD, Cobden PM, Somogyi P. Cholecystokinin-immunopositive basket and Schaffer collateral-associated interneurones target different domains of pyramidal cells in the CA1 area of the rat hippocampus. Neuroscience 2002;109:63–80. [PubMed: 11784700]

Cowell RM, Blake KR, Russell JW. Localization of the transcriptional coactivator PGC-1alpha to GABAergic neurons during maturation of the rat brain. J Comp Neurol 2007;502:1–18. [PubMed: 17335037]

Craig AM, Kang Y. Neurexin-neuroligin signaling in synapse development. Curr Opin Neurobiol 2007;17:43–52. [PubMed: 17275284]

Craig AM, Banker G, Chang W, McGrath ME, Serpinskaya AS. Clustering of gephyrin at GABAergic but not glutamatergic synapses in cultured rat hippocampal neurons. J Neurosci 1996;16:3166–3177. [PubMed: 8627355]

Craig AM, Graf ER, Linhoff MW. How to build a central synapse: clues from cell culture. Trends Neurosci 2006;29:8–20. [PubMed: 16337695]

Dalva MB, McClelland AC, Kayser MS. Cell adhesion molecules: signalling functions at the synapse. Nat Rev Neurosci 2007;8:206–220. [PubMed: 17299456]

Danglot L, Triller A, Marty S. The development of hippocampal interneurons in rodents. Hippocampus 2006;16:1032–1060. [PubMed: 17094147]

Davis EK, Zou Y, Ghosh A. Wnts acting through canonical and noncanonical signaling pathways exert opposite effects on hippocampal synapse formation. Neural Dev 2008;3:32. [PubMed: 18986540]

DeFreitas MF, Yoshida CK, Frazier WA, Mendrick DL, Kypta RM, Reichardt LF. Identification of integrin alpha 3 beta 1 as a neuronal thrombospondin receptor mediating neurite outgrowth. Neuron 1995;15:333–343. [PubMed: 7544141]

Egles C, Claudepierre T, Manglapus MK, Champliaud MF, Brunken WJ, Hunter DD. Laminins containing the beta2 chain modulate the precise organization of CNS synapses. Mol Cell Neurosci 2007;34:288–298. [PubMed: 17189701]

Ehlers MD. Activity level controls postsynaptic composition and signaling via the ubiquitin-proteasome system. Nat Neurosci 2003;6:231–242. [PubMed: 12577062]

El-Husseini AE, Schnell E, Chetkovich DM, Nicoll RA, Bredt DS. PSD-95 involvement in maturation of excitatory synapses. Science 2000;290:1364–1368. [PubMed: 11082065]

Ferreira A. Abnormal synapse formation in agrin-depleted hippocampal neurons. J Cell Sci 1999;112(Pt 24):4729–4738. [PubMed: 10574720]

Fogel AI, Akins MR, Krupp AJ, Stagi M, Stein V, Biederer T. SynCAMs organize synapses through heterophilic adhesion. J Neurosci 2007;27:12516–12530. [PubMed: 18003830]

Fox MA. Novel roles for collagens in wiring the vertebrate nervous system. Curr Opin Cell Biol 2008;20:508–513. [PubMed: 18573651]

Fox MA, Sanes JR. Synaptotagmin I and II are present in distinct subsets of central synapses. J Comp Neurol 2007;503:280–296. [PubMed: 17492637]

Fox MA, Umemori H. Seeking long-term relationship: axon and target communicate to organize synaptic differentiation. J Neurochem 2006;97:1215–1231. [PubMed: 16638017]

Fox MA, Colello RJ, Macklin WB, Fuss B. Phosphodiesterase-Ialpha/autotaxin: a counteradhesive protein expressed by oligodendrocytes during onset of myelination. Mol Cell Neurosci 2003;23:507–519. [PubMed: 12837632]

Fox MA, Alexander JK, Afshari FS, Colello RJ, Fuss B. Phosphodiesterase-I alpha/autotaxin controls cytoskeletal organization and FAK phosphorylation during myelination. Mol Cell Neurosci 2004;27:140–150. [PubMed: 15485770]

Fox MA, Sanes JR, Borza DB, Eswarakumar VP, Fassler R, Hudson BG, John SW, Ninomiya Y, Pedchenko V, Pfaff SL, Rheault MN, Sado Y, Segal Y, Werle MJ, Umemori H. Distinct target-derived signals organize formation, maturation, and maintenance of motor nerve terminals. Cell 2007;129:179–193. [PubMed: 17418794]

Freund TF, Buzsaki G. Interneurons of the hippocampus. Hippocampus 1996;6:347–470. [PubMed: 8915675]

Freund TF, Gulyas AI. Inhibitory control of GABAergic interneurons in the hippocampus. Can J Physiol Pharmacol 1997;75:479–487. [PubMed: 9250381]

Fuentealba P, Begum R, Capogna M, Jinno S, Marton LF, Csicsvari J, Thomson A, Somogyi P, Klausberger T. Ivy cells: a population of nitric-oxide-producing, slow-spiking GABAergic neurons and their involvement in hippocampal network activity. Neuron 2008;57:917–929. [PubMed: 18367092]

Gallyas F. Silver staining of collagen and reticulin fibres and crebral capillaries by means of physical development. J Microsc 1970;91:119–124. [PubMed: 4193537]

Gautam M, Noakes PG, Moscoso L, Rupp F, Scheller RH, Merlie JP, Sanes JR. Defective neuromuscular synaptogenesis in agrin-deficient mutant mice. Cell 1996;85:525–535. [PubMed: 8653788]

Gerrow K, El-Husseini A. Cell adhesion molecules at the synapse. Front Biosci 2006;11:2400–2419. [PubMed: 16720322]

Gulyas AI, Hajos N, Freund TF. Interneurons containing calretinin are specialized to control other interneurons in the rat hippocampus. J Neurosci 1996;16:3397–3411. [PubMed: 8627375]

Hall AC, Lucas FR, Salinas PC. Axonal remodeling and synaptic differentiation in the cerebellum is regulated by WNT-7a signaling. Cell 2000;100:525–535. [PubMed: 10721990]

Hashimoto T, Wakabayashi T, Watanabe A, Kowa H, Hosoda R, Nakamura A, Kanazawa I, Arai T, Takio K, Mann DM, Iwatsubo T. CLAC: a novel Alzheimer amyloid plaque component derived from a transmembrane precursor, CLAC-P/collagen type XXV. EMBO J 2002;21:1524–1534. [PubMed: 11927537]

Henkemeyer M, Itkis OS, Ngo M, Hickmott PW, Ethell IM. Multiple EphB receptor tyrosine kinases shape dendritic spines in the hippocampus. J Cell Biol 2003;163:1313–1326. [PubMed: 14691139]

Henriquez JP, Webb A, Bence M, Bildsoe H, Sahores M, Hughes SM, Salinas PC. Wnt signaling promotes AChR aggregation at the neuromuscular synapse in collaboration with agrin. Proc Natl Acad Sci U S A 2008;105:18812–18817. [PubMed: 19020093]

Herzog E, Takamori S, Jahn R, Brose N, Wojcik SM. Synaptic and vesicular co-localization of the glutamate transporters VGLUT1 and VGLUT2 in the mouse hippocampus. J Neurochem 2006;99:1011–1018. [PubMed: 16942593]

Hilgenberg LG, Su H, Gu H, O'Dowd DK, Smith MA. Alpha3Na+/K+-ATPase is a neuronal receptor for agrin. Cell 2006;125:359–369. [PubMed: 16630822]

Howard A, Tamas G, Soltesz I. Lighting the chandelier: new vistas for axo-axonic cells. Trends Neurosci 2005;28:310–316. [PubMed: 15927687]

Huang Z, Shimazu K, Woo NH, Zang K, Muller U, Lu B, Reichardt LF. Distinct roles of the beta 1-class integrins at the developing and the mature hippocampal excitatory synapse. J Neurosci 2006;26:11208–11219. [PubMed: 17065460]

Hubert T, Grimal S, Carroll P, Fichard-Carroll A. Collagens in the developing and diseased nervous system. Cell Mol Life Sci 2009;66:1223–1238. [PubMed: 19031044]

Hunt CA, Schenker LJ, Kennedy MB. PSD-95 is associated with the postsynaptic density and not with the presynaptic membrane at forebrain synapses. J Neurosci 1996;16:1380–1388. [PubMed: 8778289]

Igarashi M, Finch PW, Aaronson SA. Characterization of recombinant human fibroblast growth factor (FGF)-10 reveals functional similarities with keratinocyte growth factor (FGF-7). J Biol Chem 1998;273:13230–13235. [PubMed: 9582367]

Imai Y, Ibata I, Ito D, Ohsawa K, Kohsaka S. A novel gene iba1 in the major histocompatibility complex class III region encoding an EF hand protein expressed in a monocytic lineage. Biochem Biophs Res Commun 1996;224:855–862.

Inoguchi K, Yoshioka H, Khaleduzzaman M, Ninomiya Y. The mRNA for alpha 1(XIX) collagen chain, a new member of FACITs, contains a long unusual 3' untranslated region and displays many unique splicing variants. J Biochem 1995;117:137–146. [PubMed: 7775380]

Jang JH, Wang F, Kan M. Heparan sulfate is required for interaction and activation of the epithelial cell fibroblast growth factor receptor-2IIIb with stromal-derived fibroblast growth factor-7. In Vitro Cell Dev Biol Anim 1997;33:819–824. [PubMed: 9466688]

Kadler KE, Baldock C, Bella J, Boot-Handford RP. Collagens at a glance. J Cell Sci 2007;120(Pt 12): 1955–1958. [PubMed: 17550969]

Kalluri R. Basement membranes: structure, assembly and role in tumour angiogenesis. Nat Rev Cancer 2003;3:422–433. [PubMed: 12778132]

Kaneko T, Fujiyama F, Hioki H. Immunohistochemical localization of candidates for vesicular glutamate transporters in the rat brain. J Comp Neurol 2002;444:39–62. [PubMed: 11835181]

Kawaguchi Y, Hama K. Physiological heterogeneity of non-pyramidal cells in rat hippocampal CA1 region. Exp Brain Res 1988;72:494–502. [PubMed: 3234499]

Khaleduzzaman M, Sumiyoshi H, Ueki Y, Inoguchi K, Ninomiya Y, Yoshioka H. Structure of the human type XIX collagen (COL19A1) gene, which suggests it has arisen from an ancestor gene of the FACIT family. Genomics 1997;45:304–312. [PubMed: 9344653]

Klausberger T, Somogyi P. Neuronal diversity and temporal dynamics: the unity of hippocampal circuit operations. Science 2008;321:53–57. [PubMed: 18599766]

Knopp A, Frahm C, Fidzinski P, Witte OW, Behr J. Loss of GABAergic neurons in the subiculum and its functional implications in temporal lobe epilepsy. Brain 2008;131(Pt 6):1516–1527. [PubMed: 18504292]

Koch M, Veit G, Stricker S, Bhatt P, Kutsch S, Zhou P, Reinders E, Hahn RA, Song R, Burgeson RE, Gerecke DR, Mundlos S, Gordon MK. Expression of type XXIII collagen mRNA and protein. J Biol Chem 2006;281:21546–21557. [PubMed: 16728390]

Kohler C, Eriksson LG, Davies S, Chan-Palay V. Co-localization of neuropeptide tyrosine and somatostatin immunoreactivity in neurons of individual subfields of the rat hippocampal region. Neurosci Lett 1987;78:1–6. [PubMed: 2886960]

Kornau HC, Schenker LT, Kennedy MB, Seeburg PH. Domain interaction between NMDA receptor subunits and the postsynaptic density protein PSD-95. Science 1995;269:1737–1740. [PubMed: 7569905]

Ksiazek I, Burkhardt C, Lin S, Seddik R, Maj M, Bezakova G, Jucker M, Arber S, Caroni P, Sanes JR, Bettler B, Ruegg MA. Synapse loss in cortex of agrin-deficient mice after genetic rescue of perinatal death. J Neurosci 2007;27:7183–7195. [PubMed: 17611272]

Kummer TT, Misgeld T, Sanes JR. Assembly of the postsynaptic membrane at the neuromuscular junction: paradigm lost. Curr Opin Neurobiol 2006;16:74–82. [PubMed: 16386415]

Kuzis K, Reed S, Cherry NJ, Woodward WR, Eckenstein FP. Developmental time course of acidic and basic fibroblast growth factors' expression in distinct cellular populations of the rat central nervous system. J Comp Neurol 1995;358:142–153. [PubMed: 7560275]

Lacaille JC, Mueller AL, Kunkel DD, Schwartzkroin PA. Local circuit interactions between oriens/alveus interneurons and CA1 pyramidal cells in hippocampal slices: electrophysiology and morphology. J Neurosci 1987;7:1979–1993. [PubMed: 3612227]

Lebbink RJ, de Ruiter T, Adelmeijer J, Brenkman AB, van Helvoort JM, Koch M, Farndale RW, Lisman T, Sonnenberg A, Lenting PJ, Meyaard L. Collagens are functional, high affinity ligands for the inhibitory immune receptor LAIR-1. J Exp Med 2006;203:1419–1425. [PubMed: 16754721]

Lesuisse C, Qiu D, Bose CM, Nakaso K, Rupp F. Regulation of agrin expression in hippocampal neurons by cell contact and electrical activity. Brain Res Mol Brain Res 2000;81:92–100. [PubMed: 11000481]

Li AJ, Suzuki S, Suzuki M, Mizukoshi E, Imamura T. Fibroblast growth factor-2 increases functional excitatory synapses on hippocampal neurons. Eur J Neurosci 2002;16:1313–1324. [PubMed: 12405992]

Libby RT, Lavallee CR, Balkema GW, Brunken WJ, Hunter DD. Disruption of laminin beta2 chain production causes alterations in morphology and function in the CNS. J Neurosci 1999;19:9399–9411. [PubMed: 10531444]

Lin W, Burgess RW, Dominguez B, Pfaff SL, Sanes JR, Lee KF. Distinct roles of nerve and muscle in postsynaptic differentiation of the neuromuscular synapse. Nature 2001;410:1057–1064. [PubMed: 11323662]

Liu SH, Wang J, Zhu DY, Fu YP, Lukowiak K, Lu YM. Generation of functional inhibitory neurons in the adult rat hippocampus. J Neurosci 2003;23:732–736. [PubMed: 12574400]

Livak KJ, Schmittgen TD. Analysis of relative gene expression data using real-time quantitative PCR and the 2(−Delta Delta C(T)) method. Methods 2001;25:402–408. [PubMed: 11846609]

Lowry OH, Gilligan DR, Katersky EM. The determination of collagen and elastin in tissues, with results obtained in various normal tissues from different species. J Biol Chem 1941;139:795–804.

Lucas FR, Salinas PC. WNT-7a induces axonal remodeling and increases synapsin I levels in cerebellar neurons. Dev Biol 1997;192:31–44. [PubMed: 9405095]

Luth HJ, Winkelmann E, Celio MR. Light- and electron microscopic localization of parvalbumin, calbindin D-28k and calretinin in the dorsal lateral geniculate nucleus of the rat. J Hirnforsch 1993;34:47–56. [PubMed: 7690790]

Markram H, Toledo-Rodriguez M, Wang Y, Gupta A, Silberberg G, Wu C. Interneurons of the neocortical inhibitory system. Nat Rev Neurosci 2004;5:793–807. [PubMed: 15378039]

Marqueze B, Boudier JA, Mizuta M, Inagaki N, Seino S, Seagar M. Cellular localization of synaptotagmin I, II, and III mRNAs in the central nervous system and pituitary and adrenal glands of the rat. J Neurosci 1995;15(1):4906–4917. [PubMed: 7623121]

Martinez A, Soriano E. Functions of ephrin/Eph interactions in the development of the nervous system: emphasis on the hippocampal system. Brain Res Brain Res Rev 2005;49:211–226. [PubMed: 16111551]

Matsumoto-Miyai K, Sokolowska E, Zurlinden A, Gee CE, Luscher D, Hettwer S, Wolfel J, Ladner AP, Ster J, Gerber U, Rulicke T, Kunz B, Sonderegger P. Coincident pre- and postsynaptic activation induces dendritic filopodia via neurotrypsin-dependent agrin cleavage. Cell 2009;136:1161–1171. [PubMed: 19303856]

McBain CJ, Fisahn A. Interneurons unbound. Nat Rev Neurosci 2001;2:11–23. [PubMed: 11253355]

Melloni RH Jr, DeGennaro LJ. Temporal onset of synapsin I gene expression coincides with neuronal differentiation during the development of the nervous system. J Comp Neurol 1994;342:449–462. [PubMed: 8021345]

Melloni RH Jr, Hemmendinger LM, Hamos JE, DeGennaro LJ. Synapsin I gene expression in the adult rat brain with comparative analysis of mRNA and protein in the hippocampus. J Comp Neurol 1993;327:507–520. [PubMed: 8440778]

Misgeld T, Kummer TT, Lichtman JW, Sanes JR. Agrin promotes synaptic differentiation by counteracting an inhibitory effect of neurotransmitter. Proc Natl Acad Sci U S A 2005;102:11088–11093. [PubMed: 16043708]

Missler M, Zhang W, Rohlmann A, Kattenstroth G, Hammer RE, Gottmann K, Südhof TC. Alpha-neurexins couple Ca2+ channels to synaptic vesicle exocytosis. Nature 2003;423:939–948. [PubMed: 12827191]

Mittelsteadt T, Seifert G, Alvarez-Baron E, Steinhauser C, Becker AJ, Schoch S. Differential mRNA expression patterns of the synaptotagmin gene family in the rodent brain. J Comp Neurol 2009;512:514–528. [PubMed: 19030179]

Molinari S, Battini R, Ferrari S, Pozzi L, Killcross AS, Robbins TW, Jouvenceau A, Billard JM, Dutar P, Lamour Y, Baker WA, Cox H, Emson PC. Deficits in memory and hippocampal long-term potentiation in mice with reduced calbindin D28K expression. Proc Natl Acad Sci U S A 1996;93:8028–8033. [PubMed: 8755597]

Mullen RJ, Buck CR, Smith AM. Neun, a neuronal specific nuclear-protein in vertebrates. Development 1992;116:201–211. [PubMed: 1483388]

Myers JC, Sun MJ, D'Ippolito JA, Jabs EW, Neilson EG, Dion AS. Human cDNA clones transcribed from an unusually high-molecular-weight RNA encode a new collagen chain. Gene 1993;123:211–217. [PubMed: 7916703]

Myers JC, Yang H, D'Ippolito JA, Presente A, Miller MK, Dion AS. The triple-helical region of human type XIX collagen consists of multiple collagenous subdomains and exhibits limited sequence homology to alpha 1(XVI). J Biol Chem 1994;269:18549–18557. [PubMed: 8034603]

Myers JC, Li D, Bageris A, Abraham V, Dion AS, Amenta PS. Biochemical and immunohistochemical characterization of human type XIX defines a novel class of basement membrane zone collagens. Am J Pathol 1997;151:1729–1740. [PubMed: 9403723]

Myers JC, Li D, Amenta PS, Clark CC, Nagaswami C, Weisel JW. Type XIX collagen purified from human umbilical cord is characterized by multiple sharp kinks delineating collagenous subdomains and by intermolecular aggregates via globular, disulfide-linked, and heparin-binding amino termini. J Biol Chem 2003;278:32047–32057. [PubMed: 12788917]

Myllyharju J, Kivirikko KI. Collagens, modifying enzymes and their mutations in humans, flies and worms. Trends Genet 2004;20:33–43. [PubMed: 14698617]

Nery S, Fishell G, Corbin JG. The caudal ganglionic eminence is a source of distinct cortical and subcortical cell populations. Nat Neurosci 2002;5:1279–1287. [PubMed: 12411960]

Nishimune H, Sanes JR, Carlson SS. A synaptic laminin-calcium channel interaction organizes active zones in motor nerve terminals. Nature 2004;432:580–587. [PubMed: 15577901]

Nishimune H, Valdez G, Jarad G, Moulson CL, Muller U, Miner JH, Sanes JR. Laminins promote postsynaptic maturation by an autocrine mechanism at the neuromuscular junction. J Cell Biol 2008;182:1201–1215. [PubMed: 18794334]

Nitkin RM, Smith MA, Magill C, Fallon JR, Yao YM, Wallace BG, McMahan UJ. Identification of agrin, a synaptic organizing protein from Torpedo electric organ. J Cell Biol 1987;105(1):2471–2478. [PubMed: 2826489]

Noakes PG, Gautam M, Mudd J, Sanes JR, Merlie JP. Aberrant differentiation of neuromuscular junctions in mice lacking s-laminin/laminin beta 2. Nature 1995;374:258–262. [PubMed: 7885444]

O'Brien RJ, Xu D, Petralia RS, Steward O, Huganir RL, Worley P. Synaptic clustering of AMPA receptors by the extracellular immediate-early gene product Narp. Neuron 1999;23:309–323. [PubMed: 10399937]

O'Brien R, Xu D, Mi R, Tang X, Hopf C, Worley P. Synaptically targeted narp plays an essential role in the aggregation of AMPA receptors at excitatory synapses in cultured spinal neurons. J Neurosci 2002;22:4487–4498. [PubMed: 12040056]

O'Connor LT, Lauterborn JC, Gall CM, Smith MA. Localization and alternative splicing of agrin mRNA in adult rat brain: transcripts encoding isoforms that aggregate acetylcholine receptors are not restricted to cholinergic regions. J Neurosci 1994;14(1):1141–1152. [PubMed: 8120616]

Oliva AA Jr, Jiang M, Lam T, Smith KL, Swann JW. Novel hippocampal interneuronal subtypes identified using transgenic mice that express green fluorescent protein in GABAergic interneurons. J Neurosci 2000;20:3354–3368. [PubMed: 10777798]

Ortega N, Werb Z. New functional roles for noncollagenous domains of basement membrane collagens. J Cell Sci 2002;115(Pt 22):4201–4214. [PubMed: 12376553]

Otey CA, Kalnoski MH, Bulinski JC. Identification and quantification of actin isoforms in vertebrate cells and tissues. J Cell Biochem 1987;34:113–124. [PubMed: 3597556]

Pang ZP, Melicoff E, Padgett D, Liu Y, Teich AF, Dickey BF, Lin W, Adachi R, Südhof TC. Synaptotagmin-2 is essential for survival and contributes to Ca2+ triggering of neurotransmitter release in central and neuromuscular synapses. J Neurosci 2006a;26:13493–13504. [PubMed: 17192432]

Pang ZP, Sun J, Rizo J, Maximov A, Südhof TC. Genetic analysis of synaptotagmin 2 in spontaneous and Ca2+-triggered neurotransmitter release. EMBO J 2006b;25:2039–2050. [PubMed: 16642042]

Parra P, Gulyas AI, Miles R. How many subtypes of inhibitory cells in the hippocampus? Neuron 1998;20:983–993. [PubMed: 9620702]

Pasterkamp RJ, Peschon JJ, Spriggs MK, Kolodkin AL. Semaphorin 7A promotes axon outgrowth through integrins and MAPKs. Nature 2003;424:398–405. [PubMed: 12879062]

Pedchenko V, Zent R, Hudson BG. Alpha(v)beta3 and alpha(v)beta5 integrins bind both the proximal RGD site and non-RGD motifs within noncollagenous (NC1) domain of the alpha3 chain of type IV collagen: implication for the mechanism of endothelia cell adhesion. J Biol Chem 2004;279:2772–2780. [PubMed: 14610079]

Pleasure SJ, Anderson S, Hevner R, Bagri A, Marin O, Lowenstein DH, Rubenstein JL. Cell migration from the ganglionic eminences is required for the development of hippocampal GABAergic interneurons. Neuron 2000;28:727–740. [PubMed: 11163262]

Price CJ, Cauli B, Kovacs ER, Kulik A, Lambolez B, Shigemoto R, Capogna M. Neurogliaform neurons form a novel inhibitory network in the hippocampal CA1 area. J Neurosci 2005;25:6775–6786. [PubMed: 16033887]

Rami A, Rabie A, Thomasset M, Krieglstein J. Calbindin-D28K and ischemic damage of pyramidal cells in rat hippocampus. J Neurosci Res 1992;31:89–95. [PubMed: 1613825]

Ramón, y; Cajal, S. Histologie du systeme nerveux de l'homme et des vertbres. Paris: Maloine; 1911.

Ramont L, Brassart-Pasco S, Thevenard J, Deshorgue A, Venteo L, Laronze JY, Pluot M, Monboisse JC, Maquart FX. The NC1 domain of type XIX collagen inhibits in vivo melanoma growth. Mol Cancer Ther 2007;6:506–514. [PubMed: 17308049]

Reif R, Sales S, Hettwer S, Dreier B, Gisler C, Wolfel J, Luscher D, Zurlinden A, Stephan A, Ahmed S, Baici A, Ledermann B, Kunz B, Sonderegger P. Specific cleavage of agrin by neurotrypsin, a synaptic protease linked to mental retardation. FASEB J 2007;21:3468–3478. [PubMed: 17586728]

Rice DS, Sheldon M, D'Arcangelo G, Nakajima K, Goldowitz D, Curran T. Disabled-1 acts downstream of Reelin in a signaling pathway that controls laminar organization in the mammalian brain. Development 1998;125:3719–3729. [PubMed: 9716537]

Salinas PC, Zou Y. Wnt signaling in neural circuit assembly. Annu Rev Neurosci 2008;31:339–358. [PubMed: 18558859]

Sanes JR, Lichtman JW. Development of the vertebrate neuromuscular junction. Annu Rev Neurosci 1999;22:389–442. [PubMed: 10202544]

Sanes JR, Yamagata M. Many paths to synaptic specificity. Annu Rev Cell Dev Biol. 2009 DOI: 10.1146/annurev.cellbio. 24.110707.175402.

Sanes JR, Marshall LM, McMahan UJ. Reinnervation of muscle fiber basal lamina after removal of myofibers. Differentiation of regenerating axons at original synaptic sites. J Cell Biol 1978;78:176–198. [PubMed: 307554]

Sano Y, Nakaya T, Pedrini S, Takeda S, Iijima-Ando K, Iijima K, Mathews PM, Itohara S, Gandy S, Suzuki T. Physiological mouse brain Abeta levels are not related to the phosphorylation state of threonine-668 of Alzheimer's APP. PLoS One 2006;1:e51. [PubMed: 17183681]

Scheiffele P. Cell-cell signaling during synapse formation in the CNS. Annu Rev Neurosci 2003;26:485–508. [PubMed: 12626697]

Seppanen A, Autio-Harmainen H, Alafuzoff I, Sarkioja T, Veijola J, Hurskainen T, Bruckner-Tuderman L, Tasanen K, Majamaa K. Collagen XVII is expressed in human CNS neurons. Matrix Biol 2006;25:185–188. [PubMed: 16387484]

Shi Y, Ethell IM. Integrins control dendritic spine plasticity in hippocampal neurons through NMDA receptor and Ca2+/ calmodulin-dependent protein kinase II-mediated actin reorganization. J Neurosci 2006;26:1813–1822. [PubMed: 16467530]

Sik A, Penttonen M, Ylinen A, Buzsaki G. Hippocampal CA1 interneurons: an in vivo intracellular labeling study. J Neurosci 1995;15:6651–6665. [PubMed: 7472426]

Sloviter RS. Calcium-binding protein (calbindin-D28k) and parvalbumin immunocytochemistry - localization in the rat hippocampus with specific reference to the selective vulnerability of hippocampal-neurons to seizure activity. J Comp Neurol 1989;280:183–196. [PubMed: 2925892]

Song JY, Ichtchenko K, Südhof TC, Brose N. Neuroligin 1 is a postsynaptic cell-adhesion molecule of excitatory synapses. Proc Natl Acad Sci U S A 1999;96:1100–1105. [PubMed: 9927700]

Stevens B, Allen NJ, Vazquez LE, Howell GR, Christopherson KS, Nouri N, Micheva KD, Mehalow AK, Huberman AD, Stafford B, Sher A, Litke AM, Lambris JD, Smith SJ, John SW, Barres BA. The classical complement cascade mediates CNS synapse elimination. Cell 2007;131:1164–1178. [PubMed: 18083105]

Südhof TC. Synaptotagmins: why so many? J Biol Chem 2002;277:7629–7632. [PubMed: 11739399]

Sumiyoshi H, Inoguchi K, Khaleduzzaman M, Ninomiya Y, Yo-shioka H. Ubiquitous expression of the alpha1(XIX) collagen gene (Col19a1) during mouse embryogenesis becomes restricted to a few tissues in the adult organism. J Biol Chem 1997;272:17104–17111. [PubMed: 9202028]

Sumiyoshi H, Laub F, Yoshioka H, Ramirez F. Embryonic expression of type XIX collagen is transient and confined to muscle cells. Dev Dyn 2001;220:155–162. [PubMed: 11169848]

Sumiyoshi H, Mor N, Lee SY, Doty S, Henderson S, Tanaka S, Yoshioka H, Rattan S, Ramirez F. Esophageal muscle physiology and morphogenesis require assembly of a collagen XIX-rich basement membrane zone. J Cell Biol 2004;166:591–600. [PubMed: 15302855]

Sund M, Vaisanen T, Kaukinen S, Ilves M, Tu H, Autio-Harmainen H, Rauvala H, Pihlajaniemi T. Distinct expression of type XIII collagen in neuronal structures and other tissues during mouse development. Matrix Biol 2001;20:215–231. [PubMed: 11470398]

Tabuchi K, Blundell J, Etherton MR, Hammer RE, Liu X, Powell CM, Sudh of TC. A neuroligin-3 mutation implicated in autism increases inhibitory synaptic transmission in mice. Science 2007;318:71–76. [PubMed: 17823315]

Terauchi, A.; Javed, D.; Toth, A.; Umemori, H. Regulation of excitatory and inhibitory synapse formation by FGF22 and FGF7. Washington, DC: Society for Neuroscience; 2008. Program number 27.3/C1. Abstract viewer/Itinerary Planner

Thomas LA, Akins MR, Biederer T. Expression and adhesion profiles of SynCAM molecules indicate distinct neuronal functions. J Comp Neurol 2008;510:47–67. [PubMed: 18615557]

Tournell CE, Bergstrom RA, Ferreira A. Progesterone-induced agrin expression in astrocytes modulates glianeuron interactions leading to synapse formation. Neuroscience 2006;141:1327–1338. [PubMed: 16777347]

Trevarrow B, Marks DL, Kimmel CB. Organization of hindbrain segments in the zebrafish embryo. Neuron 1990;4:669–679. [PubMed: 2344406]

Truett GE, Heeger P, Mynatt RL, Truett AA, Walker JA, Warman ML. Preparation of PCR-quality mouse genomic DNA with hot sodium hydroxide and tris (HotSHOT). Biotechniques 2000;29:52–54. [PubMed: 10907076]

Ullrich B, Li C, Zhang JZ, McMahon H, Anderson RG, Geppert M, Südhof TC. Functional properties of multiple synaptotagmins in brain. Neuron 1994;13:1281–1291. [PubMed: 7993622]

Ullrich B, Ushkaryov YA, Südhof TC. Cartography of neurexins: more than 1000 isoforms generated by alternative splicing and expressed in distinct subsets of neurons. Neuron 1995;14:497–507. [PubMed: 7695896]

Umemori H, Sanes JR. Signal regulatory proteins (SIRPS) are secreted presynaptic organizing molecules. J Biol Chem 2008;283:34053–34061. [PubMed: 18819922]

Umemori H, Linhoff MW, Ornitz DM, Sanes JR. FGF22 and its close relatives are presynaptic organizing molecules in the mammalian brain. Cell 2004;118:257–270. [PubMed: 15260994]

Varea E, Nacher J, Blasco-Ibanez JM, Gomez-Climent MA, Castillo-Gomez E, Crespo C, Martinez-Guijarro FJ. PSA-NCAM expression in the rat medial prefrontal cortex. Neuroscience 2005;136:435–443. [PubMed: 16216431]

Vaughn JE. Fine structure of synaptogenesis in the vertebrate central nervous system. Synapse 1989;3:255–285. [PubMed: 2655146]

Veit G, Kobbe B, Keene DR, Paulsson M, Koch M, Wagener R. Collagen XXVIII, a novel von Willebrand factor A domain-containing protein with many imperfections in the collagenous domain. J Biol Chem 2006;281:3494–3504. [PubMed: 16330543]

Vogel W, Gish GD, Alves F, Pawson T. The discoidin domain receptor tyrosine kinases are activated by collagen. Mol Cell 1997;1:13–23. [PubMed: 9659899]

Webb DJ, Zhang H, Majumdar D, Horwitz AF. alpha5 integrin signaling regulates the formation of spines and synapses in hippocampal neurons. J Biol Chem 2007;282:6929–6935. [PubMed: 17213186]

Wendland B, Miller KG, Schilling J, Scheller RH. Differential expression of the p65 gene family. Neuron 1991;6:993–1007. [PubMed: 2054189]

Wichterle H, Turnbull DH, Nery S, Fishell G, Alvarez-Buylla A. In utero fate mapping reveals distinct migratory pathways and fates of neurons born in the mammalian basal forebrain. Development 2001;128:3759–3771. [PubMed: 11585802]

Xu NJ, Henkemeyer M. Ephrin-B3 reverse signaling through Grb4 and cytoskeletal regulators mediates axon pruning. Nat Neurosci 2009;12:268–276. [PubMed: 19182796]

Xu Q, Cobos I, De La Cruz E, Rubenstein JL, Anderson SA. Origins of cortical interneuron subtypes. J Neurosci 2004;24:2612–2622. [PubMed: 15028753]

Xu X, Roby KD, Callaway EM. Mouse cortical inhibitory neuron type that coexpresses somatostatin and calretinin. J Comp Neurol 2006;499:144–160. [PubMed: 16958092]

Yamagata M, Weiner JA, Sanes JR. Sidekicks: synaptic adhesion molecules that promote lamina-specific connectivity in the retina. Cell 2002;110:649–660. [PubMed: 12230981]

Yamagata M, Sanes JR, Weiner JA. Synaptic adhesion molecules. Curr Opin Cell Biol 2003;15:621–632. [PubMed: 14519398]

Yoshioka H, Zhang H, Ramirez F, Mattei MG, Moradi-Ameli M, van der Rest M, Gordon MK. Synteny between the loci for a novel FACIT-like collagen locus (D6S228E) and alpha 1 (IX) collagen (COL9A1) on 6q12-q14 in humans. Genomics 1992;13:884–886. [PubMed: 1639419]

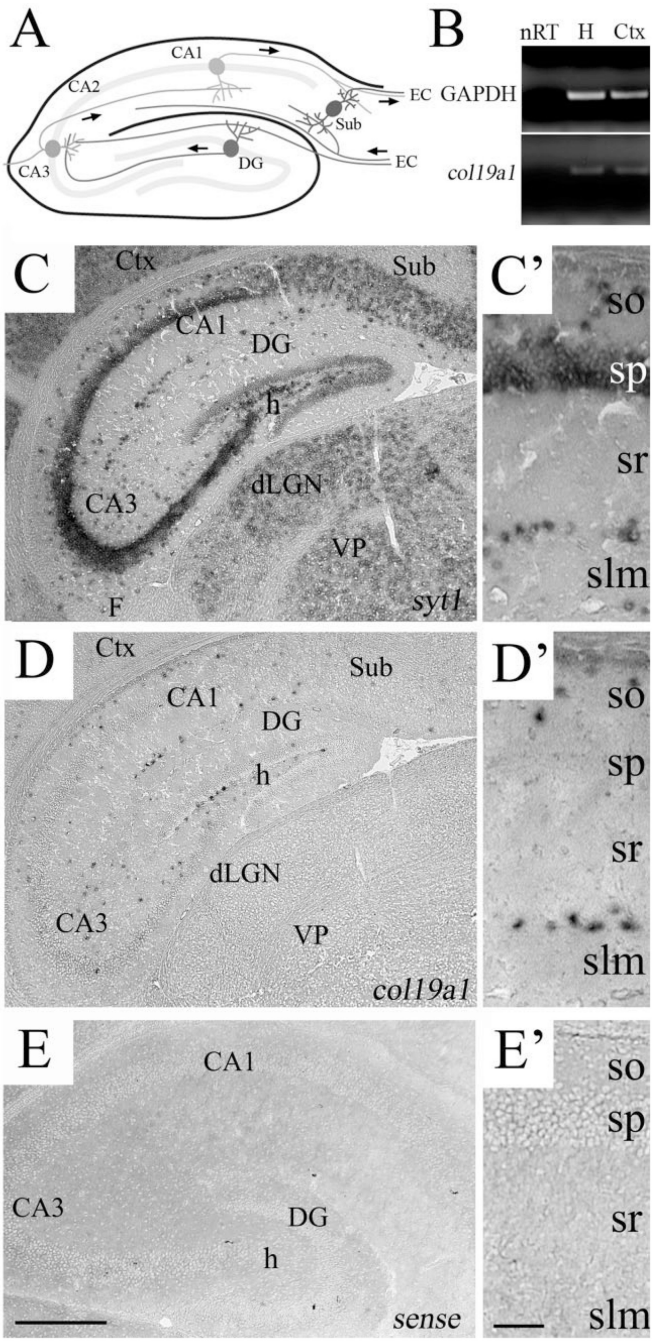

Figure 1.

Col19a1 expression in the mammalian hippocampus. **A**: Schematic representation of the unidirectional excitatory circuit within the mouse hippocampus. Interneurons not depicted. Arrows indicate the direction of information flow. **B**: RT-PCR analysis demonstrated the presence of *col19a1* mRNA in hippocampus and cortex at P14. Glyceraldehyde 3-phosphate dehydrogenase (*gapdh*) was a loading control and a sample containing hippocampal RNA but no reverse transcriptase (nRT) was a negative control. **C,D**: Localization of *syt1* (C) and *col19a1* (D)mRNAs by in situ hybridization in P14 mouse hippocampus. C',D',E' show high magnification images of CA1 regions. C,C': Syt1 mRNA demonstrates the location of hippocampal neurons. D,D': *Col19a1* mRNA is sparsely distributed in hippocampus and

cortex. Note the absence of *col19a1* mRNA expression in other regions of the mouse brain, i.e., dLGN and VP. **E,E'** Sense controls for *col19a1* riboprobes. CA, Cornu Ammonis areas; DG, dentate gyrus; dLGN, dorsal lateral geniculate nucleus; EC, enthorinal cortex; h, hilus; slm, stratum lacunosum-moleculare; so, stratum oriens; sp, stratum pyramidalis; sr, stratum radiatum; Sub, subiculum; VP, ventral posterior thalamic nucleus. Scale bars = 400 μm in E (applies to C–E); 100 μm in E' (applies to C'–E').

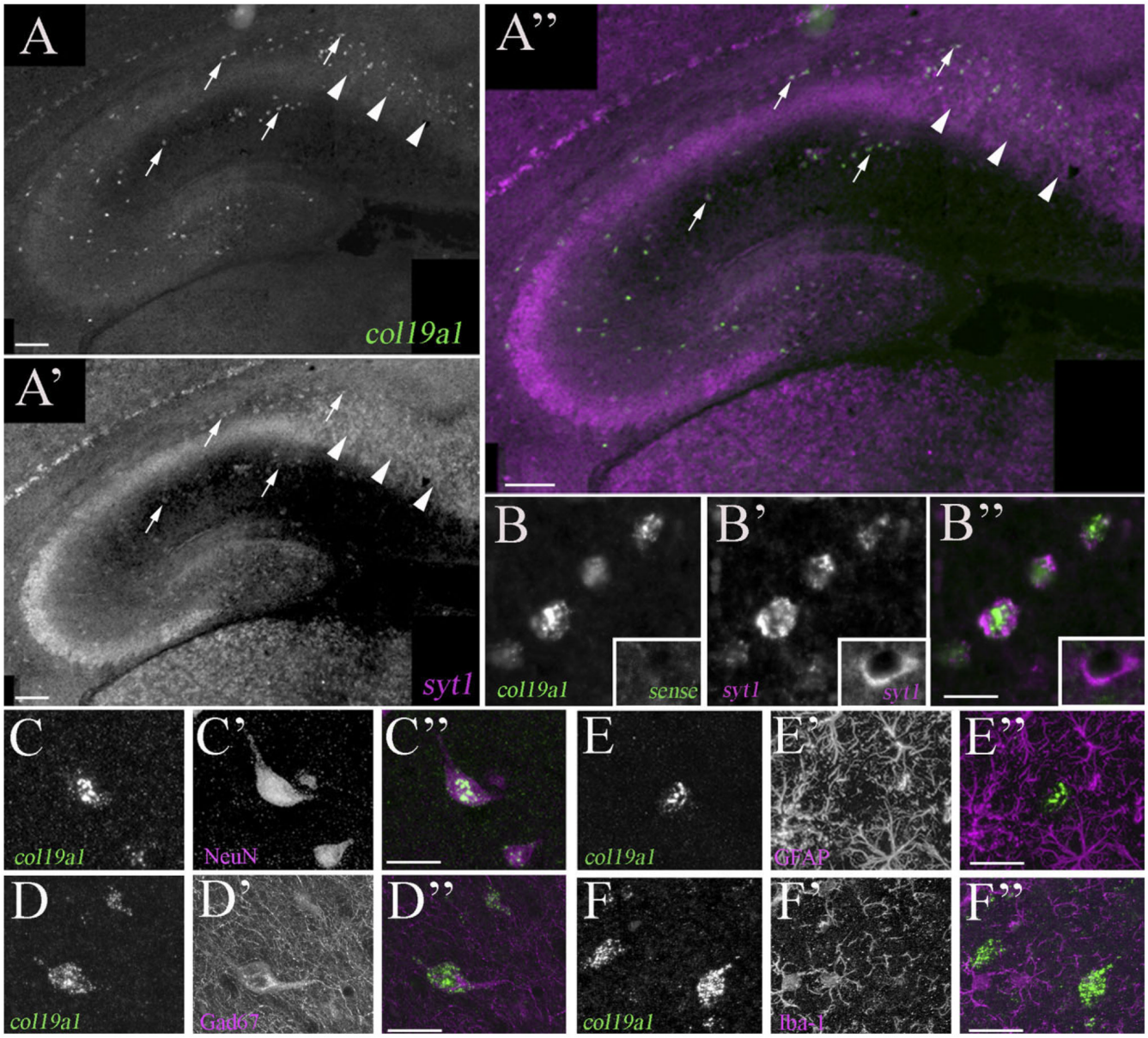

Figure 2.

Col19a1 is expressed by neurons. **A**: D-FISH for *col19a1* (green) and *syt1* (magenta) in P7 mouse hippocampus. Arrows indicate examples of *col19a1* and *syt1* coexpression. Arrowheads highlight subiculum. **B**: High magnification of neurons coexpressing *syt1* and *col19a1* mRNAs. Inset shows *col19a1* sense control riboprobes combined with *syt1* riboprobes. **C**: Expression of *col19a1* by neurons was verified with NeuN immunolabeling. **D**: FISH-IHC revealed *col19a1* mRNA was present in Gad67-immunoreactive interneurons. **E,F**: Neither hippocampal astrocytes, labeled with GFAP antibodies (E), or microglia, labeled with Iba-1 antibodies (F), contained *col19a1* mRNA. Label colors in black and white image panels correspond to the color of that image in the multicolored composite image. Scale bars = 200 μm in A,A',A"; 25 μm in C"-F".

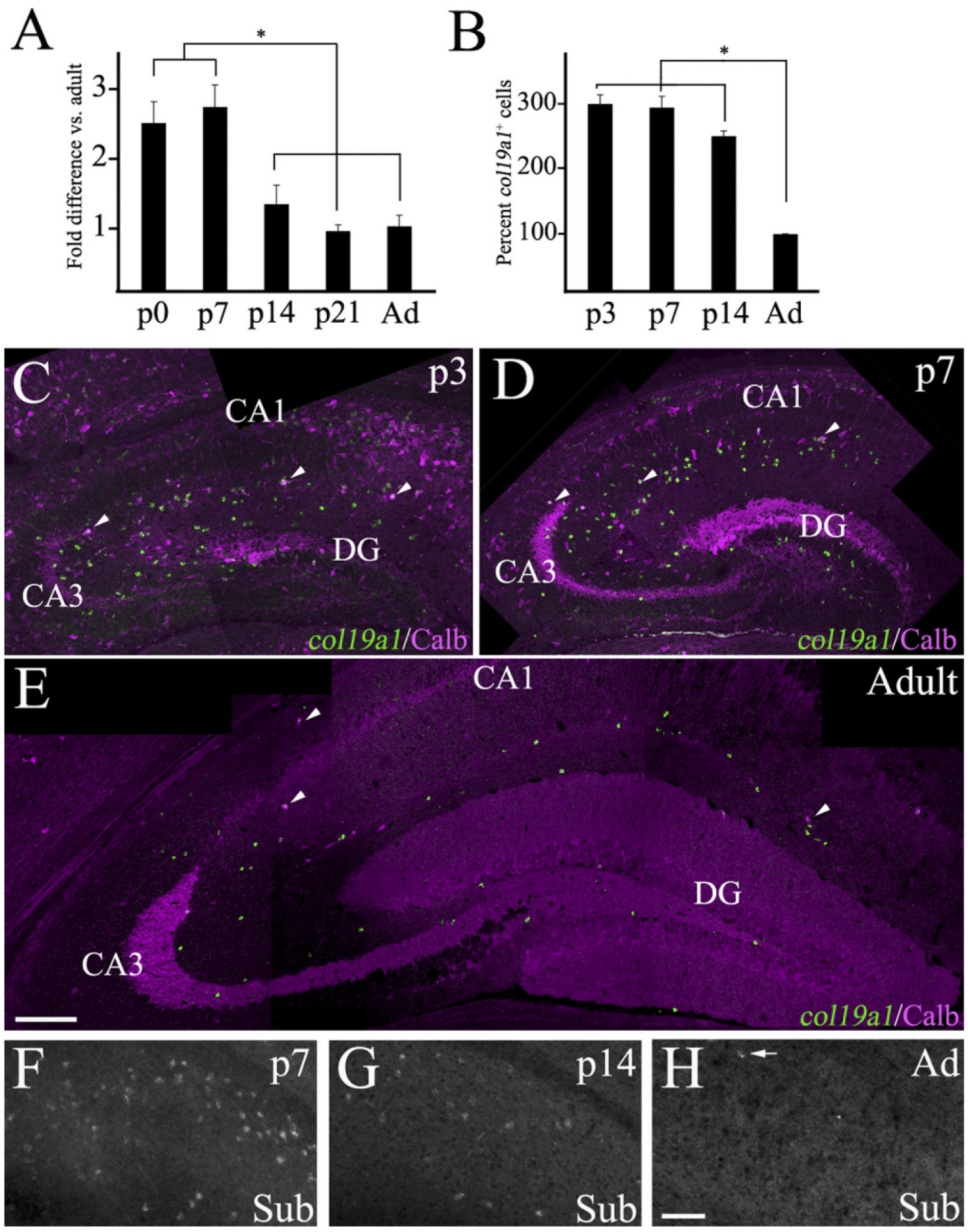

Figure 3.

Developmental regulation of *col19a1* in hippocampus. **A**: Quantitative RT-PCR demonstrates highest levels of hippocampal *col19a1* mRNA at P0 and P7. Levels of *col19a1* were normalized to *gapdh*. $n = 3$ in triplicate. *Differs from P14, P21 and adult samples at $P < 0.001$ by Holm-Sidak one-way analysis of variance (ANOVA). **B**: Relative numbers of *col19a1*-expressing cells, labeled by in situ hybridization, compared to adult levels. Similar regions of hippocampus were compared between ages. *Differs from adult samples at $P < 0.001$ by Holm-Sidak one-way ANOVA. **C–E**: Examples of in situ hybridization for *col19a1* mRNA (green) at P3 (C), P7 (D), and adult (E). Note the higher density of *col19a1*-expressing cells at P3 and P7. Sections were costained with antibodies against Calb (magenta) to identify hippocampal regions. Arrowheads in C–E demonstrate coexpression of Calb and *col19a1* mRNA. **F–H**: In subiculum, ISH revealed *col19a1* expression peaked at P7 (F) and was dramatically decreased by P14(G) and in adult samples (H). This is

markedly different from other regions of the hippocampus, where expression continues into adulthood (E). Arrow in H indicates *col19a1*-expressing cell in adult subiculum. Scale bars = 200 μm in E (applies to C–E); 100 μm in H (applies to F–H).

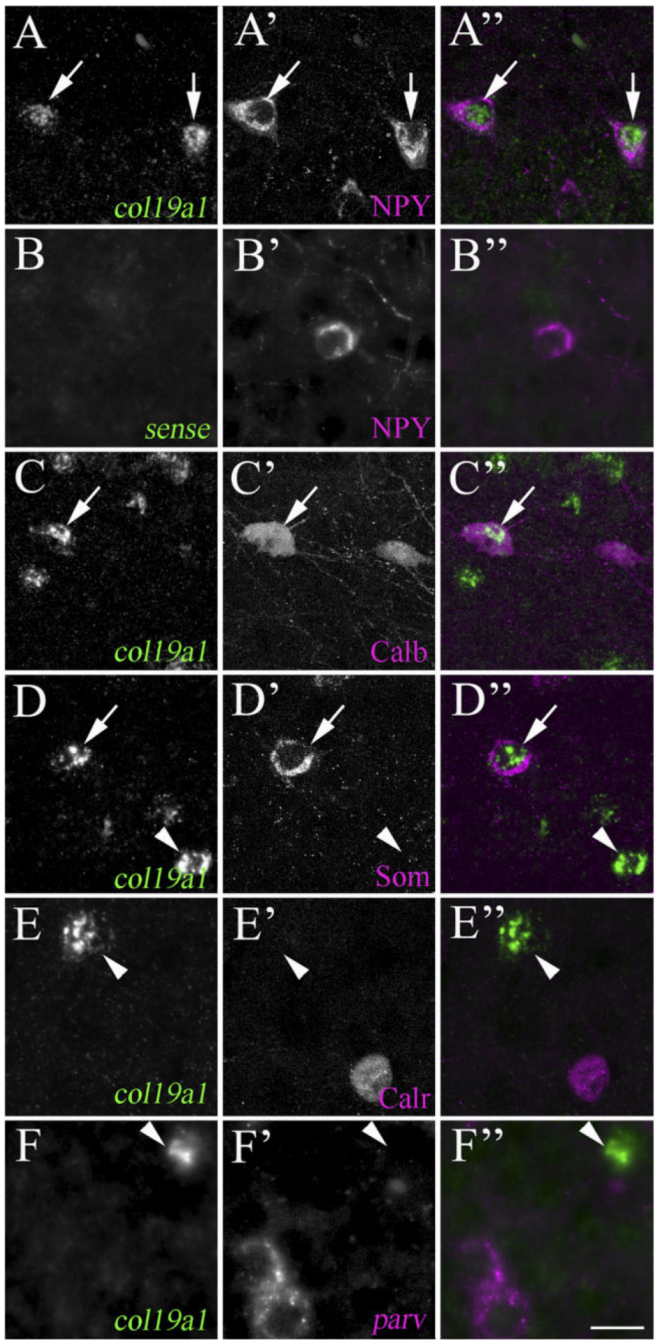

Figure 4.

Distinct subclasses of hippocampal interneurons express *col19a1* mRNA. **A–D**: FISH-IHC demonstrated subsets of NPY-(A), Calb-(C), and Som-(D) immunoreactive interneurons express *col19a1* mRNA. B shows *col19a1* sense control riboprobes combined with NPY IHC. **E**: FISH-IHC revealed Calr-immunoreactive neurons do not express *col19a1*. **F**: D-FISH demonstrated *col19a1* and *parv*, which encodes parvalbumin, are not coexpressed in hippocampus. Arrows indicate examples of coexpression of *col19a1*. Arrowheads indicate *col19a1*-expressing cells not labeled with the interneuron marker. Label colors in black and white image panels correspond to the color of that image in the multicolored composite image. Scale bar = 25 μm.

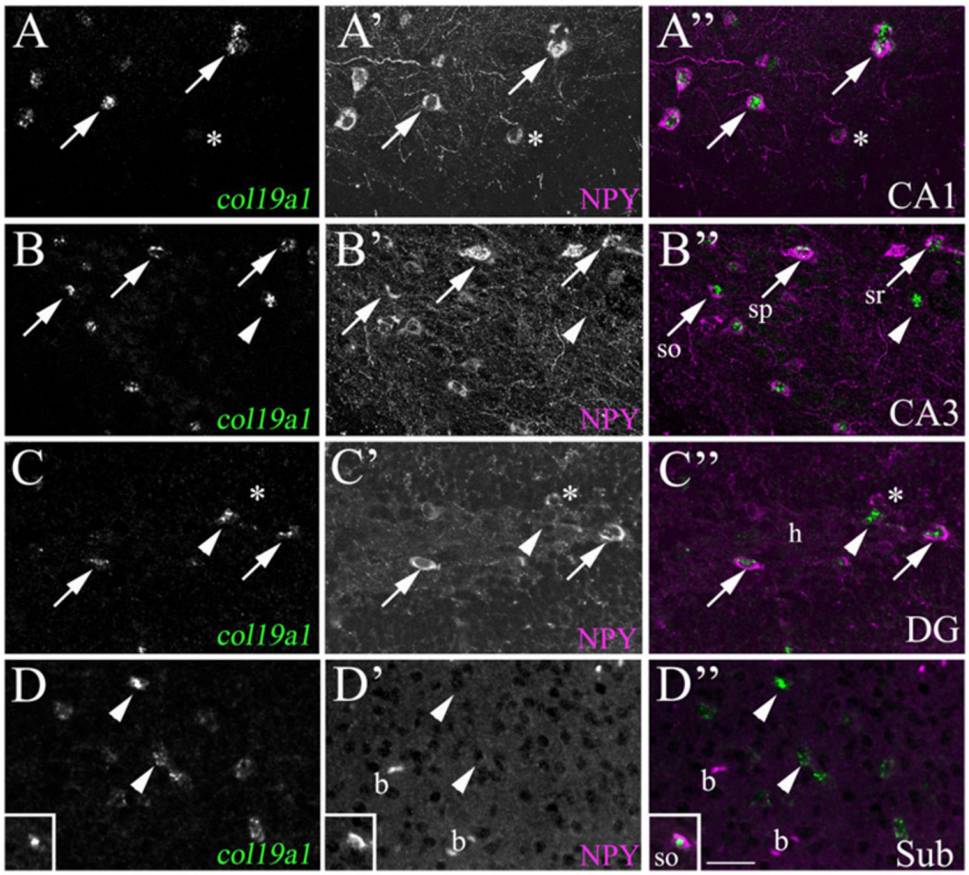

Figure 5.

Regional coexpression of *col19a1* mRNA and NPY in the developing hippocampus. In situ hybridization for *col19a1* mRNA (green) and immunostaining for NPY (magenta) in P14 hippocampus. **A–C**: Most *col19a1*-expressing neurons in CA1 (A), CA3 (B), and the hilus of the DG (C) contain NPY. In CA1 and CA3 coexpression of *col19a1* and NPY was seen in all layers (see arrows in B). **D**: In subiculum, *col19a1*-expressing cells do not contain NPY. Inset in D shows *col19a1*-NPY coexpressing neuron in stratum oriens of CA1 adjacent to the same section of subiculum. Arrows highlight examples of *col19a1* and NPY coexpression. Arrowheads indicate *col19a1*-expressing cells that do not contain NPY. Asterisks indicate NPY-immunoreactive neurons that lack *col19a1* mRNA. “b” labels nonspecific immunoreactivity associated with blood vessels. CA, Cornu Ammonis areas; DG, dentate gyrus; h, hilus; so, stratum oriens; sp, stratum pyramidalis; sr, stratum radiatum; Sub, subiculum. Label colors in black and white image panels correspond to the color of that image in the multicolored composite image. Scale bar = 50 μm.

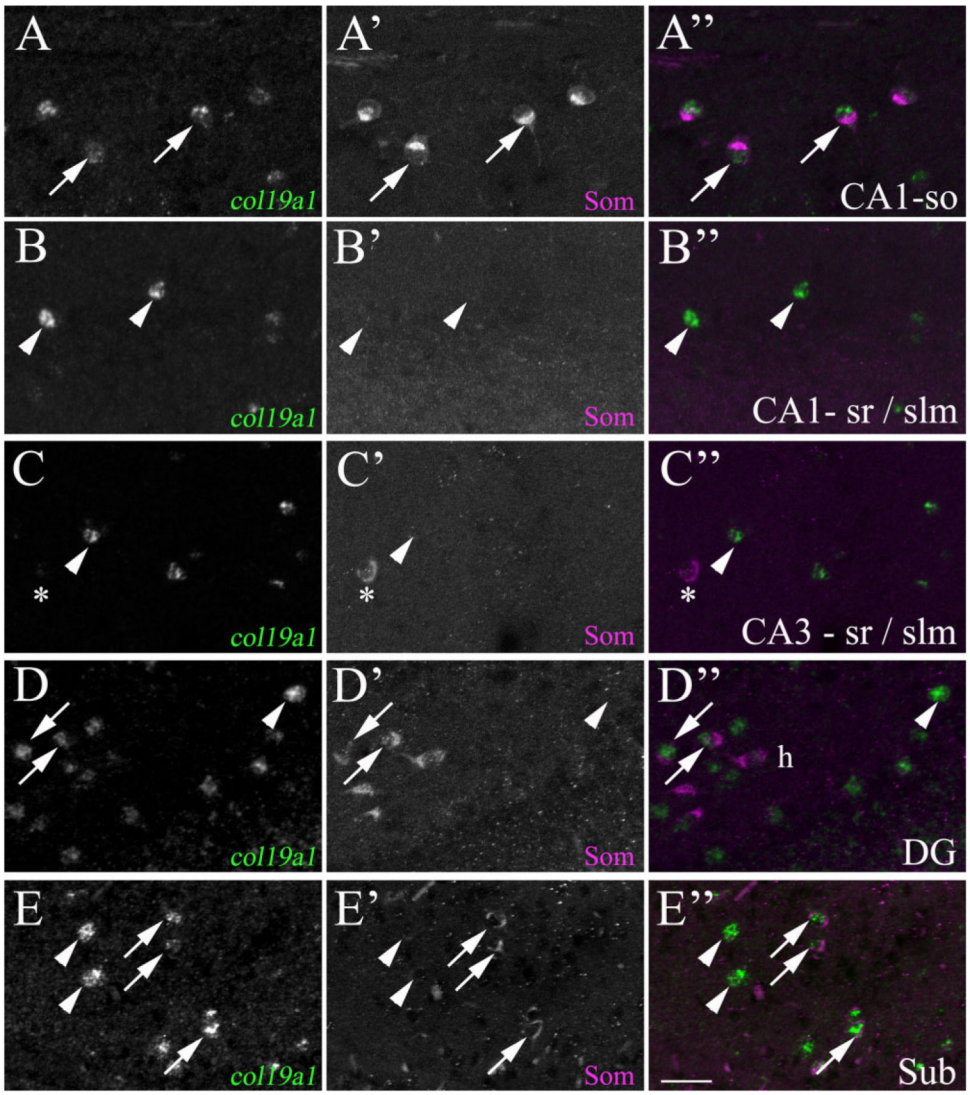

Figure 6.

Regional coexpression of *col19a1* mRNA and Som in the developing hippocampus. In situ hybridization for *col19a1* mRNA (green) and immunostaining for Som (magenta) in P14 hippocampus. **A**: *Col19a1*-expressing neurons in stratum oriens of CA1 (A) contain Som. **B,C**: *Col19a1*-expressing cells in strata pyramidalis, radiatum, and lacunosum-moleculare do not contain Som. **D,E**: Many *col19a1*-expressing cells in the hilus of the DG (D) and subiculum (E) contain Som. Arrows highlight examples of *col19a1* and Som coexpression. Arrowheads indicate *col19a1*-expressing cells that do not contain Som. Asterisks indicate Som-immunoreactive neurons that lack *col19a1* mRNA. CA, Cornu Ammonis areas; DG, dentate gyrus; h, hilus; so, stratum oriens; sp, stratum pyramidalis; sr, stratum radiatum; Sub, subiculum. Label colors in black and white image panels correspond to the color of that image in the multicolored composite image. Scale bar = 50 μm.

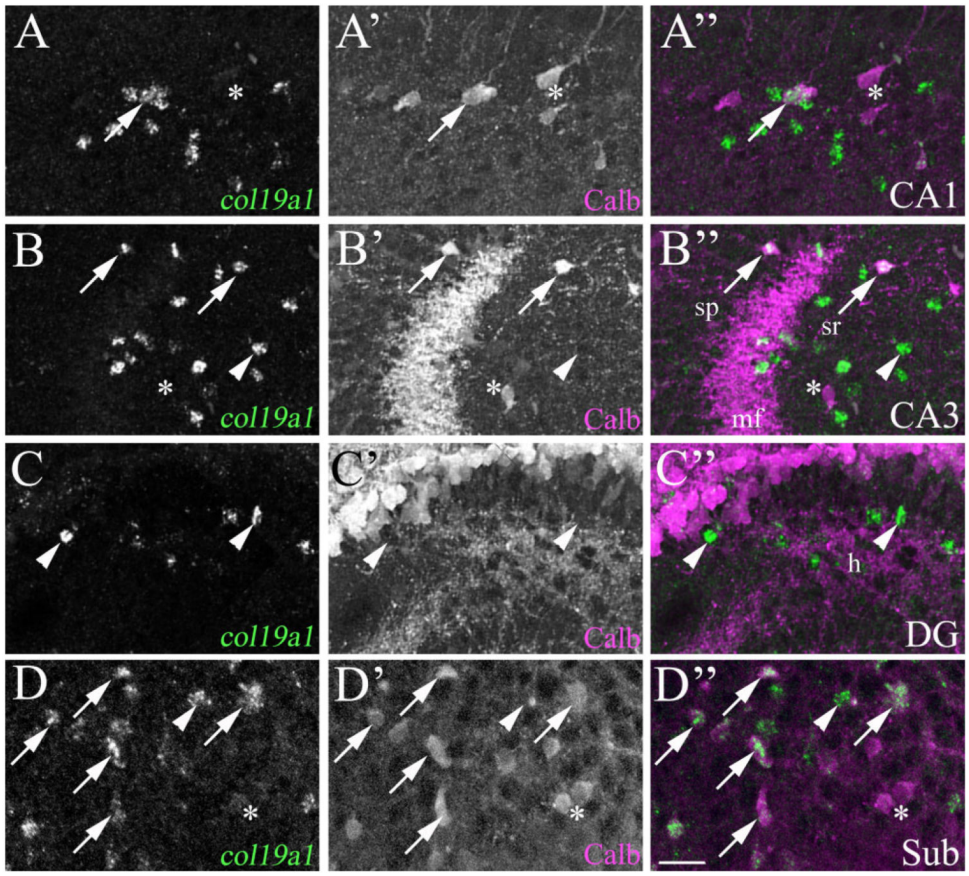

Figure 7.

Regional coexpression of *col19a1* mRNA and Calb in the developing hippocampus. ISH for *col19a1* mRNA (green) and immunostaining for Calb (magenta) in P7 hippocampus. **A–C**: Sparse coexpression of *col19a1* mRNA and Calb was observed in CA1 (A), CA3 (B), and the hilus of the DG (C). **D**: Many *col19a1*-expressing cells in subiculum contained Calb. Arrows highlight examples of *col19a1* and calbindin coexpression. Asterisks indicate Calb-immunoreactive neurons that lack *col19a1* mRNA. Arrowheads indicate *col19a1*-expressing cells that do not contain calbindin. CA, Cornu Ammonis areas; DG, dentate gyrus; h, hilus; mf, mossy fiber terminals; so, stratum oriens; sp, stratum pyramidalis; sr, stratum radiatum; Sub, subiculum. Label colors in black and white image panels correspond to the color of that image in the multicolored composite image. Scale bar = 50 μm.

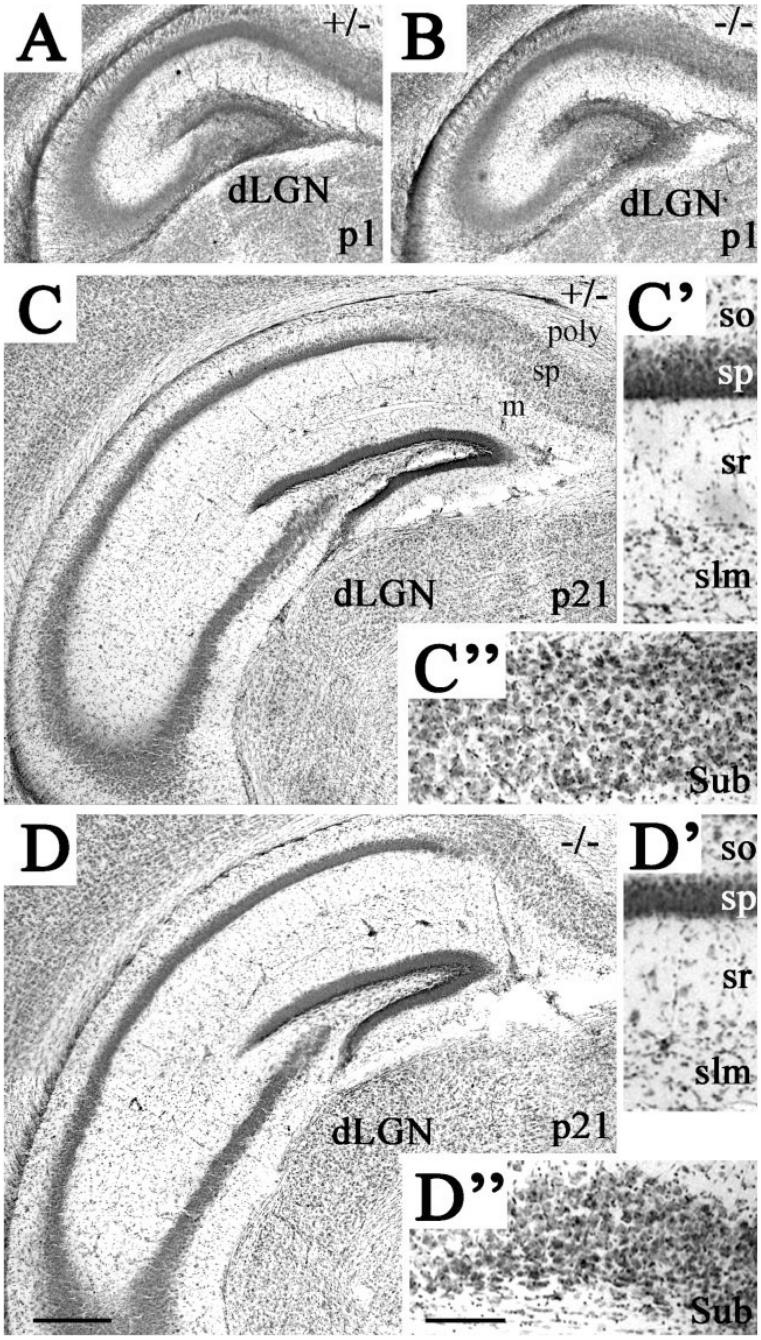

Figure 8.

Normal morphological development of the brain occurs in the absence of collagen XIX. Micrographs of cresyl violet stained hippocampi from P1 (**A,B**)andP21 (**C,D**) *col19a1*$^{-/-}$ mutants (−/−; B,D) and littermate controls (+ /− A,C). Mutant hippocampi at both ages were slightly smaller than littermate controls; however, differences in size were not specific to the hippocampus; regions that normally lack *col19a1* mRNA were similarly smaller in mutant brains (see dLGN). C',D' show high magnification of CA1. C",D" show high magnification of stratum pyramidalis of subiculum. m, molecular layer; poly, polymorphic layer; so, stratum oriens; sp, stratum pyramidalis; sr, stratum radiatum; slm, stratum

lacunosum-moleculare; Sub, subiculum. Scale bars = 400 μm in D (applies to A–D); 200 μm in D” (applies to C’,C”,D’,D”).

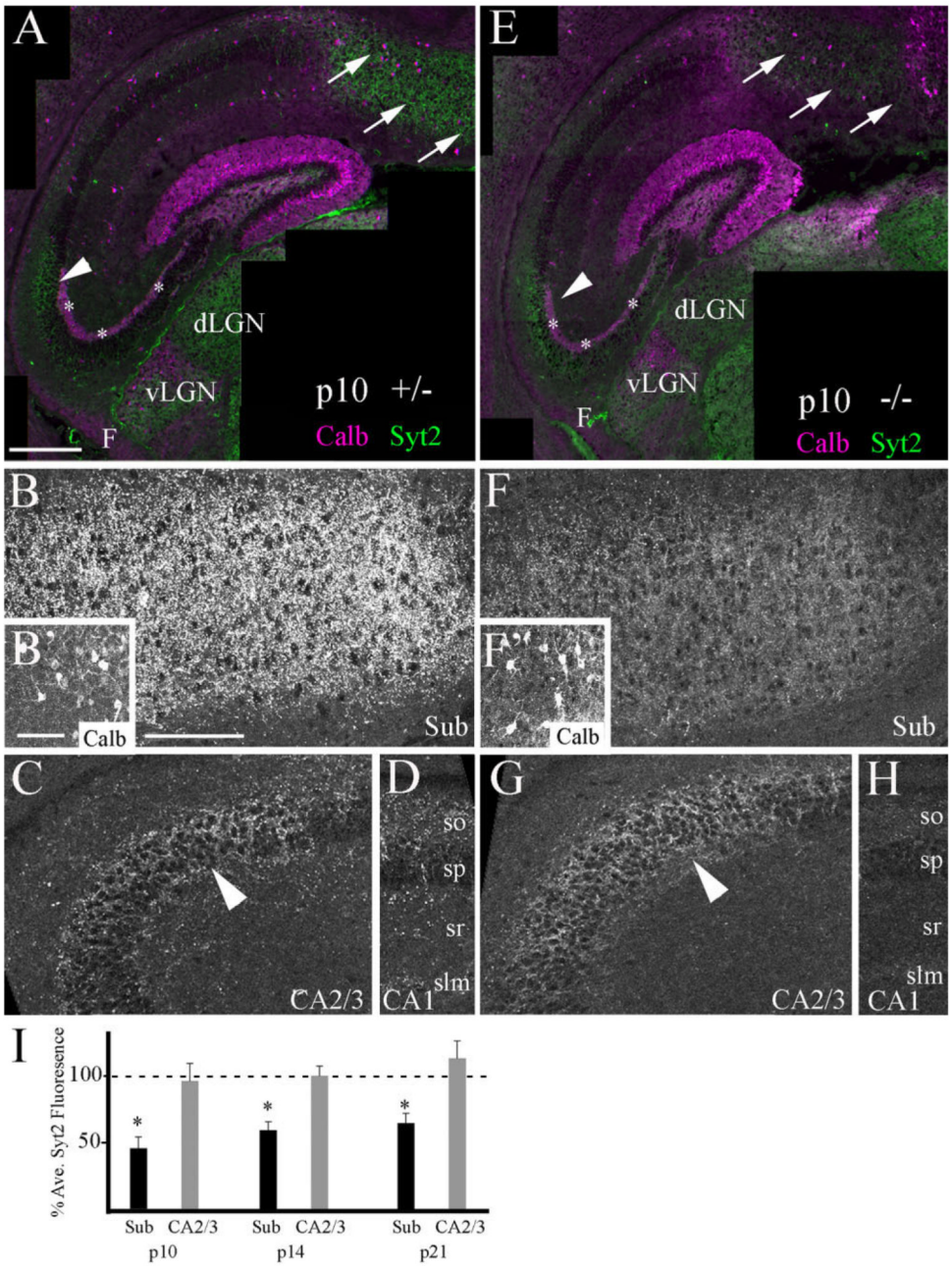

Figure 9.

Collagen XIX is required for the normal formation of synaptic terminals in subiculum. **A–D**: IHC for Syt2 (green) in P10 control (+ / −) hippocampi. At this age Syt2-positive nerve terminals were present in subiculum (see B and arrows in A), stratum pyramidalis of CA2 and CA3 (see C and arrowhead in A) and sparsely distributed terminals throughout the synaptic layers of all other CA regions (D) **E–H**: Drastically reduced levels of Syt2-immunoreactive nerve terminals were detected in *col19a1*$^{-/-}$ mutant (−/−) subiculum. Defects were specific to subiculum (see F and arrows in E) and the sparsely distributed terminals in synaptic layers of CA1 and CA3 (H). Syt2-positive nerve terminals in stratum pyramidalis of CA2 and CA3 were present in normal numbers in mutant hippocampi (see G and arrowhead in E). B,F show high-magnification confocal image of Syt2-

immunoreactivity in control (B)and mutant (F) P10 subiculum. B',F'show corresponding Calb-immunoreactivity in control (B)and mutant (F) P10 subiculum in same regions shown in B,F. C,G show high-magnification confocal image of Syt2-immunoreactivity in control (C)and mutant (G) P10 CA2/CA3 regions. D,H show high-magnification confocal image of Syt2-immunoreactivity in control (D) and mutant (H) P10 CA1. A,E,B',F': Calb-immunoreactivity (magenta) label hippocampal interneurons (in A,E,B',F'), interneurons within vLGN (in A,E) and DG granular cells and mossy fibers (in A,E; asterisks indicate mossy fibers). Only sections containing vLGN, dLGN, and fimbria hippocampus (f) were analyzed. Mutant and control images acquired with identical settings. **I**: Quantification of average fluorescent intensities of Syt2-IHC in mutants and controls were compared in subiculum and CA2/CA3 regions. Dashed line represent control levels. Data shown are ± SEM; $n > 6$. *Differs from control, age-matched subiculum at $P < 0.01$ by Student's *t*-test. Scale bars = 400 μm in A (applies to A,E); 200 μm in B (applies to B–D,F–H); 100 μm in B' (applies to F').

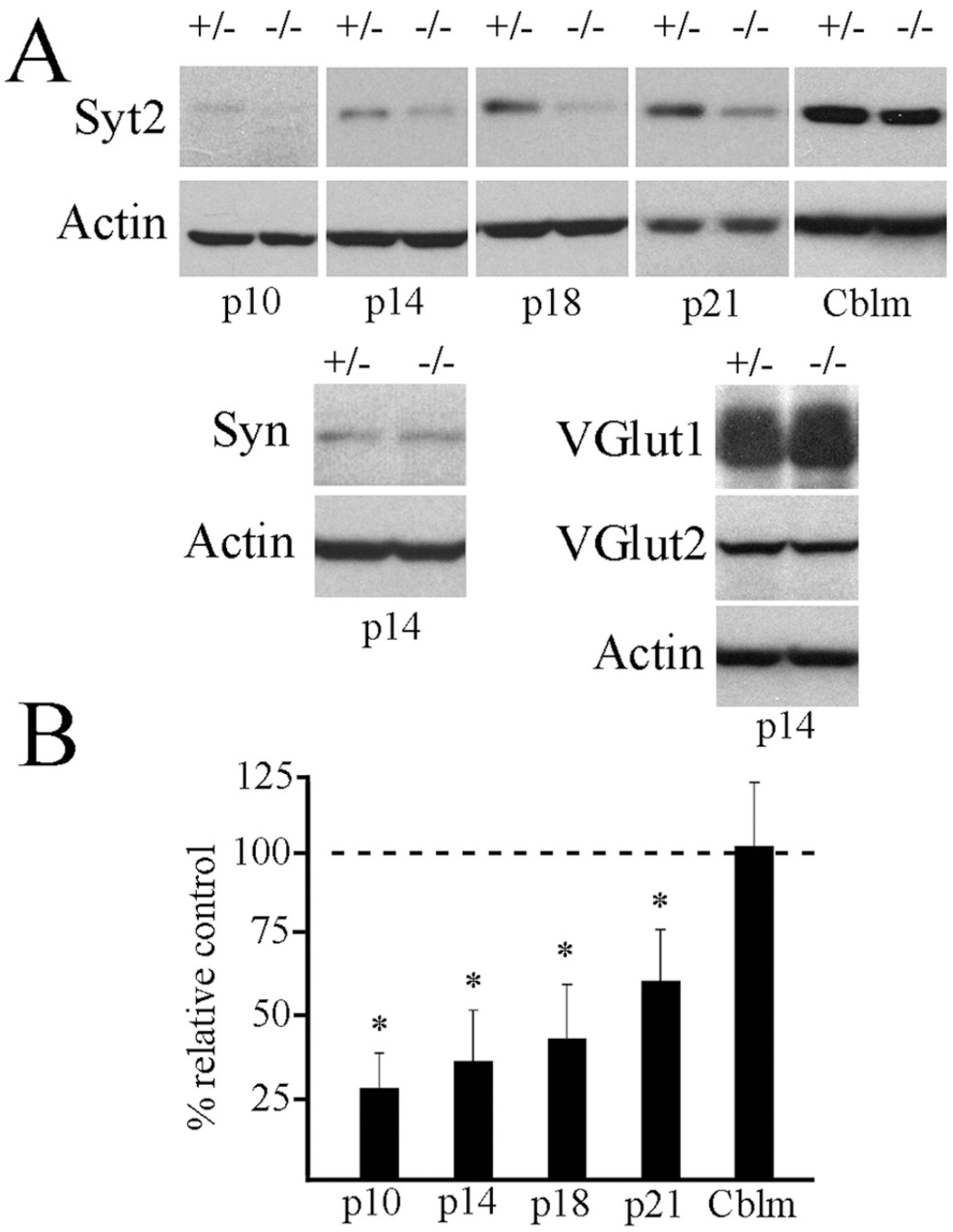

Figure 10.

Decreased levels of Syt2 in collagen XIX-deficient hippocampi. **A**: Western blots demonstrate reduced Syt2 levels in P10, P14, P18, and P21 mutant (−/−) hippocampal extracts compared to littermate controls (+/ −). No differences were observed for synap-sin (Syn), vesicular glutamate transporter 1 (VGlut1), or VGlut2. Nor were differences observed in Syt2 levels observed in mutant cerebella (Cblm), which normally lack *col19a1* mRNA. Levels of actin were used as loading controls. **B**: Quantification of hippocampal and cerebellar Syt2 protein levels detected by Western blot and normalized to actin. Dashed line represents control levels. Data shown are ± SEM; n= 3. *Differs from control age-matched sample at $P < 0.05$ by Student's t-test.

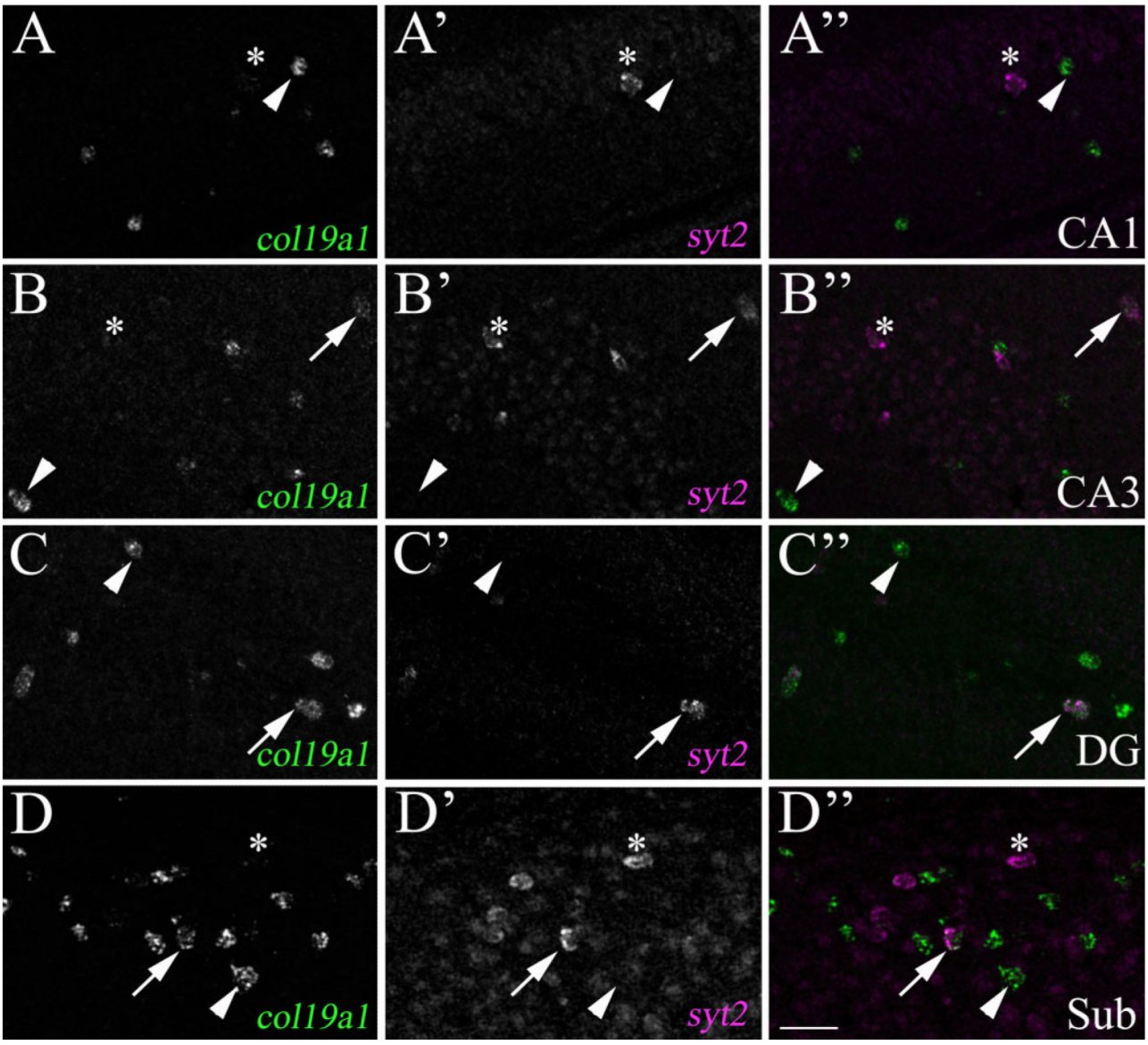

Figure 11.

Regional coexpression of *col19a1* and *syt2* mRNA in the developing hippocampus. In situ hybridization for *col19a1* mRNA (green) and *syt2* mRNA (magenta) in P14 hippocampus. **A,B**: Most *col19a1*-expressing neurons in CA1 (A) and CA3 (B)do not coexpress *syt2* mRNA (but see arrow in B). C: In the hilusof the DG, all *syt2*-expressiong neurons expressed *col19a1* mRNA (see arrow in C); however, many *col19a1*-expressing neurons lacked *syt2* mRNA (arrowheads). D: In subiculum, many cells expressed one of these genes (see asterisks and arrowhead). However, a small population of *col19a1*-expressing cells contained *syt2* mRNA, and vice versa (arrow in D). Arrows highlight examples of *col19a1* and *syt2* coexpression. Arrowheads indicate *col19a1*-expressing cells that lack *syt2* mRNA. Asterisks indicate *syt2*-expressing neurons that lack *col19a1* mRNA. CA, Cornu Ammonis areas; DG, dentate gyrus; h, hilus; so, stratum oriens; sp, stratum pyramidalis; sr, stratum radiatum; Sub, subiculum. Label colors in black and white image panels correspond to the color of that image in the multicolored composite image. Scale bar = 50 μm.

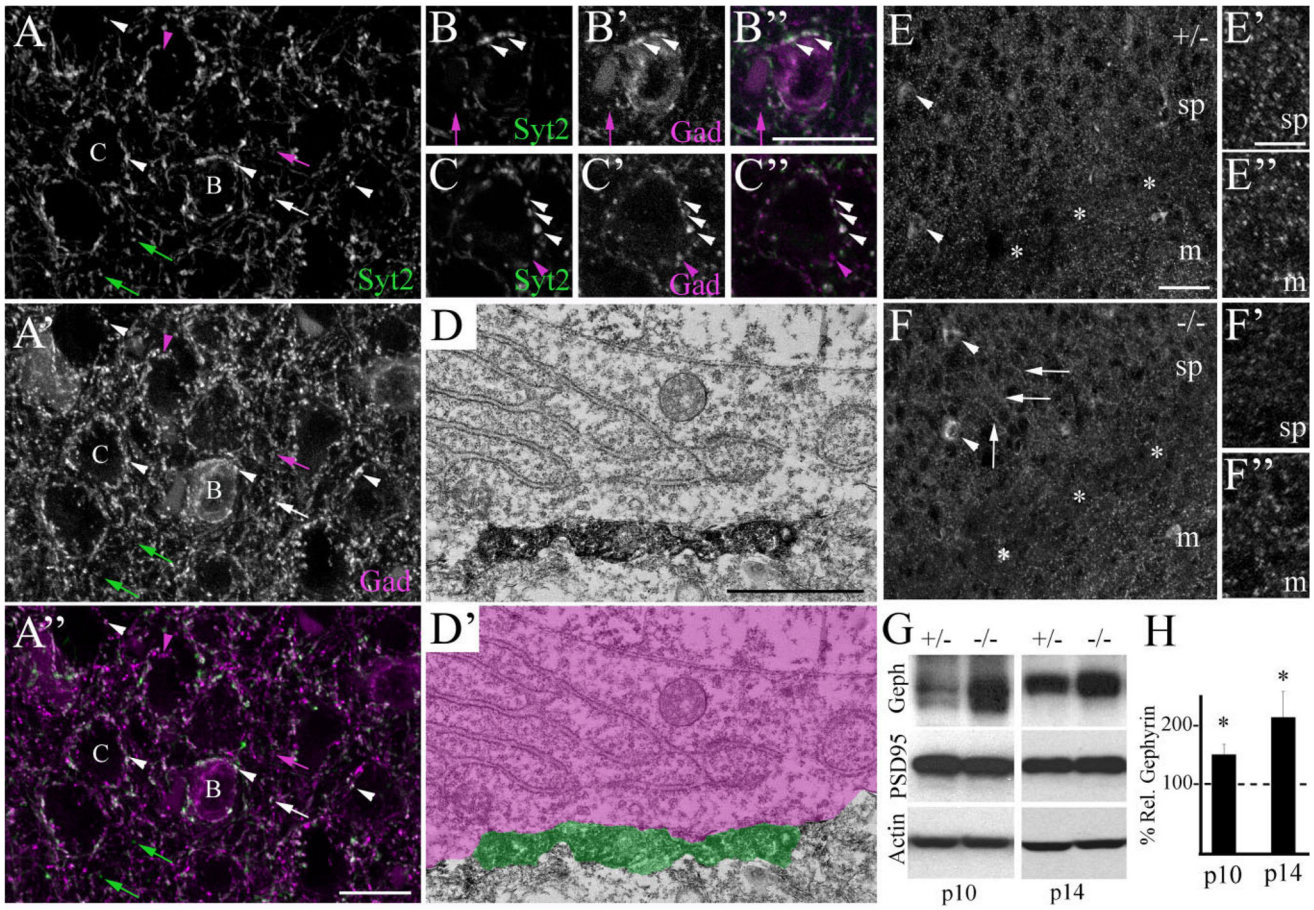

Figure 12.

Collagen XIX is required for the formation of inhibitory synapses in the developing subiculum. **A–C**: IHC for Syt2 (green) and Gad65/67 (magenta) in wildtype P14 subiculum. Most Syt2-containing synapses contained Gad65/67, including both axo-somatic synapses (white arrowheads) and synapses not associated with cell bodies (white arrows). However, not all Gad65/67-immunoreactive synapses contained Syt2 (magenta arrows and arrowheads). A small population of Syt2-immunoreactive synapses lacked Gad65/67 (green arrows). In A, "B" and "C" denote regions enlarged in B and C, respectively. B,C: High-magnification images demonstrating colocalization of Gad65/67 and Syt2 in axo-somatic synapses (white arrowheads). In B, inhibitory axo-somatic synapses are present on the soma of a Gad65/67-immunoreactive inhibitory interneuron. In A–C, arrowheads denote axo-somatic synapses and arrows depict synapses not associated with cell somas. White arrows or arrowheads depict colocalization of Syt2 and Gad65/67, whereas those colored magenta or green highlight synapses containing only Gad65/67 or Syt2, respectively. **D**: Electron micrograph of a Syt2-positive axo-somatic inhibitory synapses in wildtype P10 subiculum. D' shows a pseudo-colored version of D: postsynaptic cell soma in magenta and DAB-labeled Syt2-positive terminal in green. **E,F**: Gad67 immunolabeling in P10 *col19a1*$^{-/-}$; mutant (−/−; F) and control (+ /−; E) subiculum. In mutant stratum pyramidalis *(sp)*, levels of Gad67 were increased in cell bodies and processes (see arrowheads and arrows, respectively) and decreased in synaptic structures compared with controls. In contrast to *sp*, reduced levels of Gad67 were not observed in the adjacent molecular layer (*m*) of mutant subiculum. Asterisks depict boundary between *sp* and *m*. E',F' show high-magnification confocal images of Gad67 labeling in control and mutant *sp*, respectively. E",F" show high-

magnification confocal images of Gad67 labeling in control and mutant *m*, respectively. **G**: Western blot analysis of gephyrin and PSD-95 in P10 and P14 *col19a1*$^{-/-}$ mutant (−/−) and control (+/−) hippocampal extracts. Levels of actin were used as loading controls. **H**: Levels of mutant gephyrin were quantified by densitometry, normalized to actin, and compared to normalized control levels. Dashed line represents control levels. Data shown are ± SEM, $n = 3$. *Differs from age-matched control at $P < 0.05$ by Student's *t*-test. Label colors in black and white image panels correspond to the color of that image in the multicolored composite image. Scale bars = 20 μm in A"; 20 μm in B" (applies to B,C); 800 nm in D; 60 μm in E (applies to F); 15 μm in E' (applies to E',E",F',F").

TABLE 1

Antibodies Used

Antigen	Isotype	Description of immunogen	Source/catalog number	Dilution for IHC	Dilution for WB
Actin	Mouse IgG1	Purified chicken gizzard actin	Chemicon #MAB1501		1:20,000
Calbindin	Rabbit polyclonal	Rat calbindin D28k	Swant, #CB-38a	1:1,000	
Calretinin	Rabbit polyclonal	Recombinant rat calretinin	Chemicon #AB5054	1:2,500	
Gephyrin	Mouse IgG1	Purified rat gephyrin	Synaptic Systems		1:1,000
Glial fibrillary acidic protein (GFAP)	Rabbit polyclonal	GFAP isolated from cow spinal cord	DAKO #Z0334	1:2,500	
Glutamate decarboxylase 67 (Gad 67)	Mouse IgG2a	Recombinant Gad67	Chemicon #MAB5406	1:1,000	
Glutamate decarboxylase 65 & 67 (Gad 65/67)	Rabbit polyclonal	Synthetic peptide containing a Cysteine residue and amino acids 572–585 of rath Gad65	Chemicon #AB1511	1:500	
Ionizing calcium-binding adaptor 1 (Iba-1)	Rabbit polyclonal	Synthetic peptide corresponding to the first 29 amino acids of Iba-1	WAKO #016–20001	1:500	
Neuronal Nuclei (NeuN)	Mouse IgG1	Purified cell nuclei from mouse brain	Chemicon #MAB377	1:200	
Neuropeptide Y (NPY)	Rabbit polyclonal	Neuropeptide Y coupled to bovine thyroglobulin	ImmunoStar #22940	1:500	
Postsynaptic density protein 95 (PSD-95)	Mouse IgG2a	Purified recombinant rat PSD-95	Affinity BioReagents		1:3,000
Somatostatin	Rabbit polyclonal	Somatostatin conjugated to BSA	Chemicon #AB5494	1:250	
Synapsin	Mouse IgG1	Purified synapsin 1	Synaptic Systems, #106001	1:500	1:100
Synaptotagmin 2	Mouse IgG2a	1–5 day zebrafish embryo	Zebrafish International Resource Center	1:200	1:100
Vesicular glutamate transporter 1 (VGlut1)	Mouse IgG1	Recombinant fusion protein consisting of amino acids 493–560 of rat VGlut1	NeuroMab; Clone N28/9		1:400
Vesicular glutamate transporter 2 (VGlut2)	Mouse IgG1	Recombinant fusion protein consisting of amino acids 501–582 of rat VGlut2	NeuroMab; Clone N29/29		1:400

TABLE 2

Summary of Coexpression of Various Neurochemicals or Genes by *col19a1*-expressing Hippocampal Interneurons

Region	NPY	Som	Calb	Calr	*parv*	*syt2*
CA1						
SO	++	+ +	+	−	−	+/ −
SP	++	−	+	−	−	+/ −
SLM	++	−	+	−	−	+/ −
SR	++	−	+	−	−	+/ −
CA3						
SO	++	++	+	−	−	+/ −
SP	++	−	+	−	−	+/ −
SLM	++	−	+	−	−	+/ −
SR	++	−	+	−	−	+/ −
DG						
GCL	−	−	−	−	−	−
H	++	+	+/−	−	−	+
Subiculum						
Poly	−	+	−	−	−	+/−
SP	−	++	++	−	−	+
M	−	−	+	−	−	−

Calb, calbindin; Calr, calretinin; GCL, granular cell layer; H, hilus; M, molecular layer; NPY, neuropeptide Y; *parv*, gene encoding parvalbumin; Poly, polymorphic layer; SLM, stratum lacunosum moleculare; SO, stratum oriens; Som, somatostatin; SP, stratum pyramidalis; SR, stratum radiatum; *syt2*, gene encoding synaptotagmin 2; '−' no coexpression observed;'+/−' only occasional coexpression observed; '+' consistent, but small, set of coexpressing cells observed; '++' large number of coexpressing cells observed.